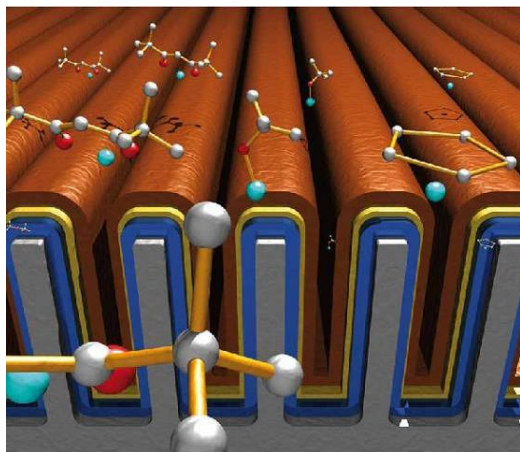
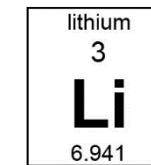


UiO : Centre for Materials Science and Nanotechnology  
University of Oslo

Ola Nilsen

# Atomic layer deposition for microbatteries



**BATLAB**

# The abstract...

All **solid state microbatteries** can only be realised using pinhole free films, particularly for the electrolytes, where also thinner is better in terms of ionic conductivity. The atomic layer deposition (ALD) technique is identified as perhaps the enabling technology for realisation of such structures, also on 3D structures.

The current contribution will give an **overview of the present status** in deposition of materials for microbatteries by ALD, with highlights from both the anodes, electrolytes and cathodes, where **recent findings in pseudocapacitive behaviour of LiFePO<sub>4</sub>** will be given. The ALD technique has traditionally been used for deposition of dielectric materials, also when it comes to ionic conductivities, while battery materials are ideally highly conducting with respect to Li-ions. This has led to **challenges in deposition processes containing lithium** where the growth perhaps no longer is strictly terminated by the surface reactions. What implications does this have on the ALD-growth?

# Reviews



EarlyView publication on wiley.com  
(issue and volume)  
DOI:



## Atomic layer deposition in energy conversion applications Chapter 6

ADVANCED MATERIALS  
www.admat.de

### Elegant design of electrode and electrolyte interface in lithium-ion batteries by atomic layer deposition

Jian Liu and Xueliang Sun<sup>1</sup>

Department of Mechanical and Materials Engineering, University of Western Ontario, London, ON,  
Canada, N6A 5B9

E-mail: xsun@eng.uwo.ca

Received 4 July 2014, revised 7 August 2014  
Accepted for publication 15 August 2014  
Published 16 December 2014

#### Abstract

Lithium-ion batteries (LIBs) are very promising power supply systems for a variety of applications, such as electric vehicles, plug-in hybrid electric vehicles, grid energy storage microelectronics. However, to realize these practical applications, many challenges need to be addressed in LIBs, such as power and energy density, cycling lifetime, safety, and cost. Atomic layer deposition (ALD) is emerging as a powerful technique for solving these problems. Exclusive advantages over other film deposition counterparts. In this review, we summarize state-of-the-art progresses of employing ALD to design novel nanostuctured electrodes and solid-state electrolytes and to tailor electrode/electrolyte interface by surface engineering in order to prevent unfavorable side reactions and achieve optimal performance of LIBs. Insights into the future research and development of the ALD technique for LIBs are also discussed. We expect that this review article will provide resourceful information for researchers in both fields of LIBs and ALD and also will stimulate more interest in using ALD for the development of next-generation LIBs.

Keywords: atomic layer deposition, lithium-ion battery, surface coating, electrode/electrolyte interface  
(Some figures may appear in colour only in the online journal)

#### 1. Introduction

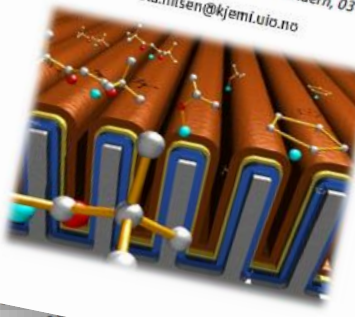
At present, there is growing awareness of the necessity to develop electric vehicles (EVs) and plug-in hybrid electric vehicles (PHEVs) in order to reduce fossil fuel dependence and improve environmental stewardship. Lithium-ion batteries (LIBs) have been considered as one of the most promising energy storage systems for EVs and PHEVs because they can offer a higher operative voltage and energy density than the other available competing technologies [1, 2]. The interest in EVs and PHEVs has stimulated research in industry and academia to develop the next generation of batteries for EVs and PHEVs that can match the performance of internal combustion vehicles, and great advances have been made.

<sup>1</sup> Author to whom any correspondence should be addressed.

0957-4484/15/024001-14\$30.00

### Atomic layer deposition for thin film lithium ion batteries

Ola Nilsen\*, Knut B. Gandraud, Amund Ruud, Helmer Fjellvåg  
Centre for Materials Science and Nanotechnology (SMN), Department of Chemistry, University of Oslo, P.O.Box 1033 Blindern, 0315 Oslo, Norway  
ola.nilsen@kjemi.uio.no



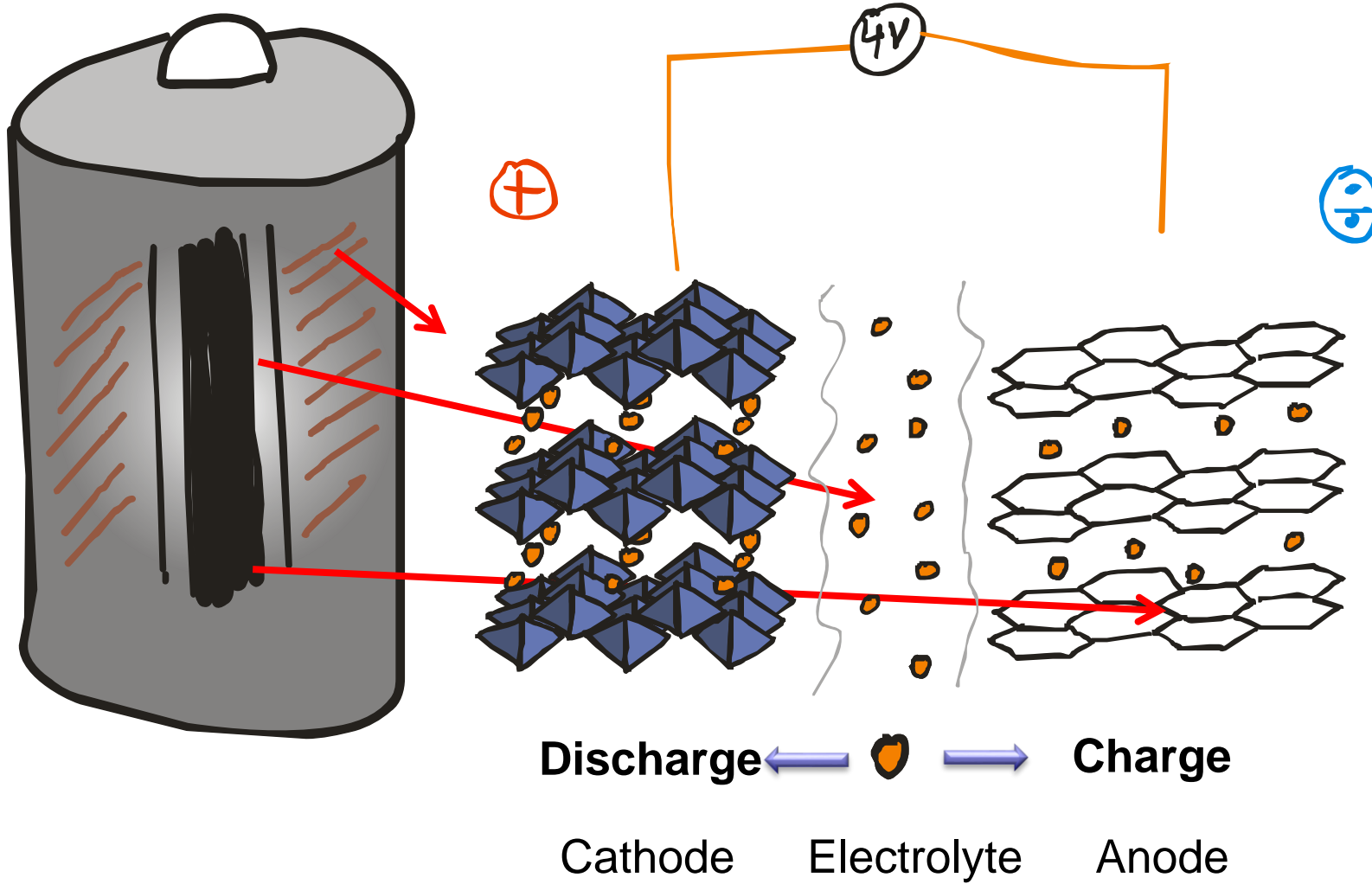
wileyonlinelibrary.com 3589

H.C.M. Knoops, ..., W.M.M. Kessels, *J. Vac. Sci. Technol. A*, **30** (2012) 010801.

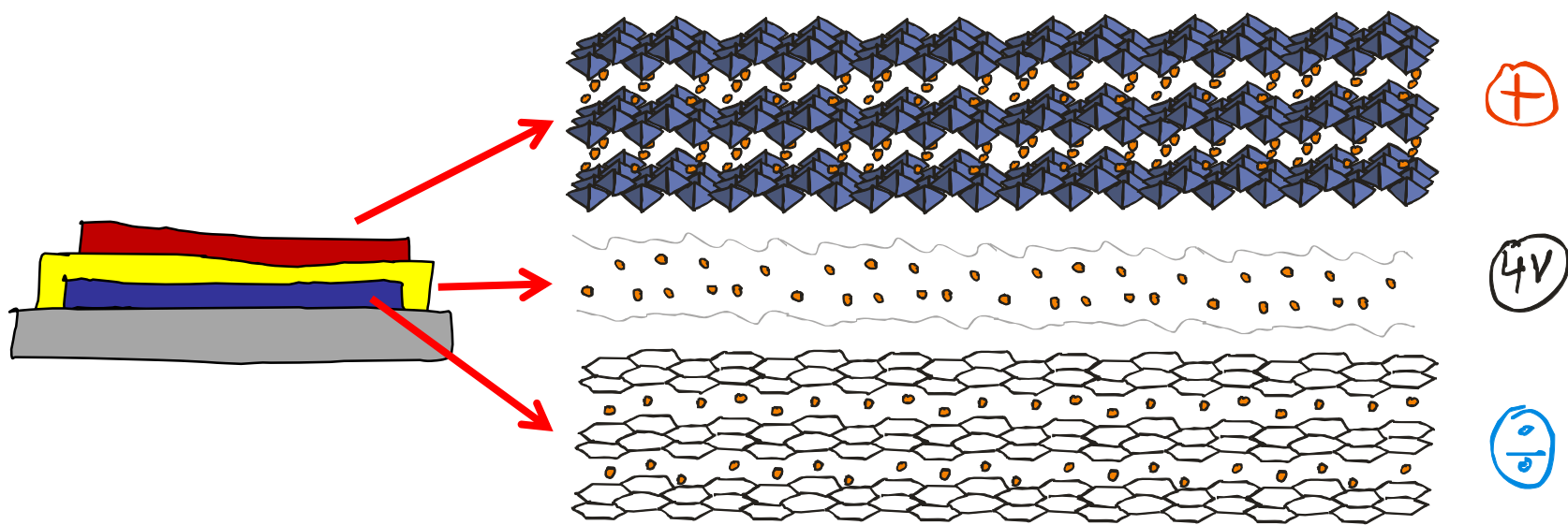
T. Aaltonen, ..., H. Fjellvåg, *ECS Transactions* **41** (2011) 331.

X. Meng, ..., X. Sun, *Advanced Materials*, **24** (2012) 3589.

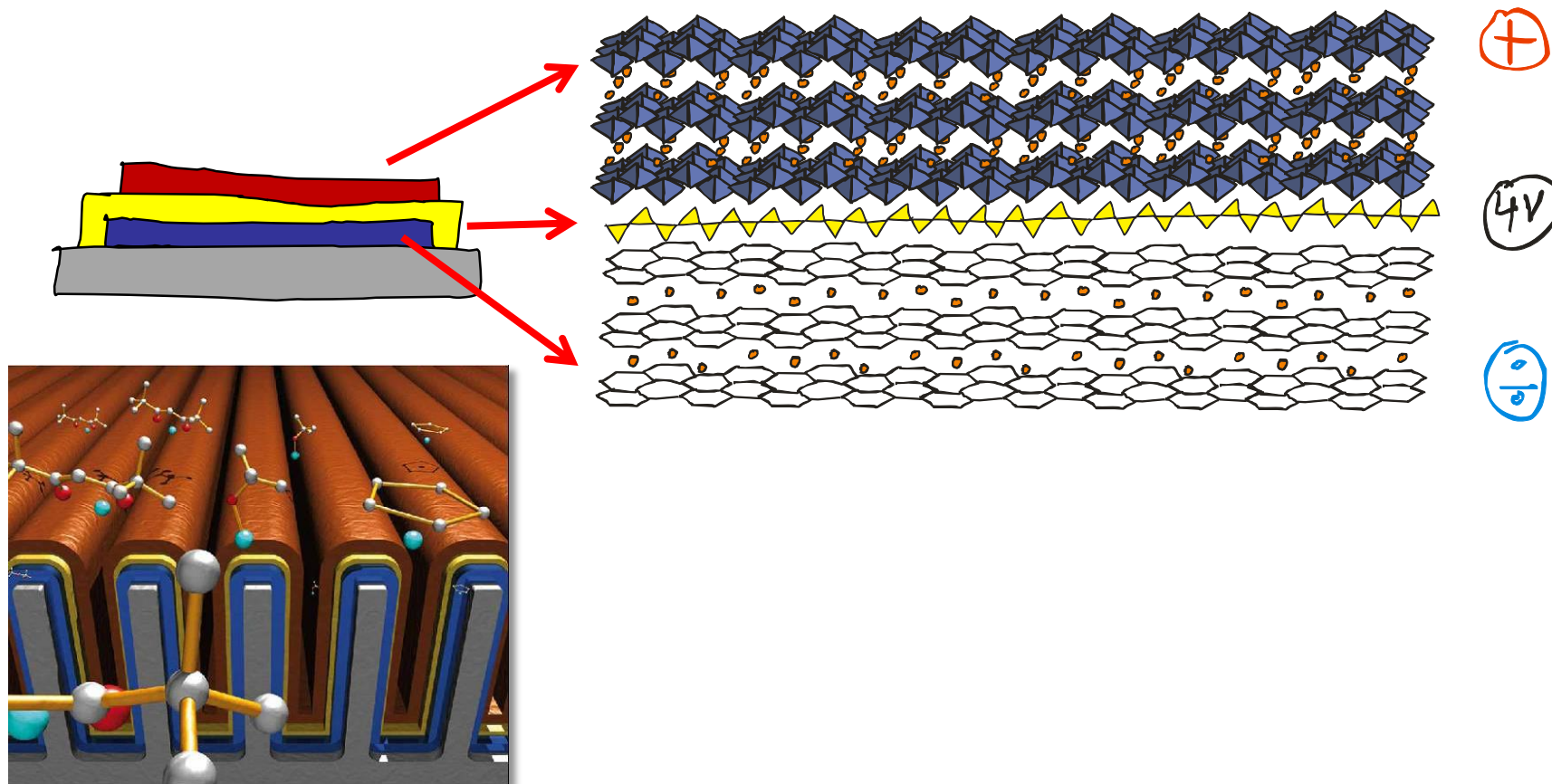
# Li-battery



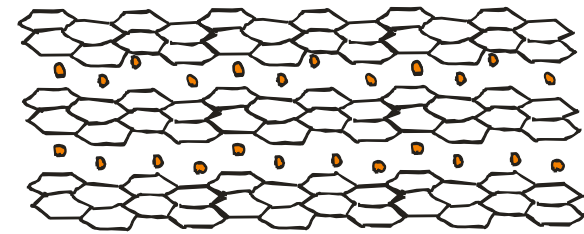
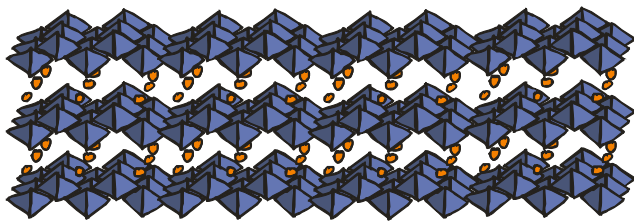
# Li-film battery



# Li-film battery



# Li-film battery

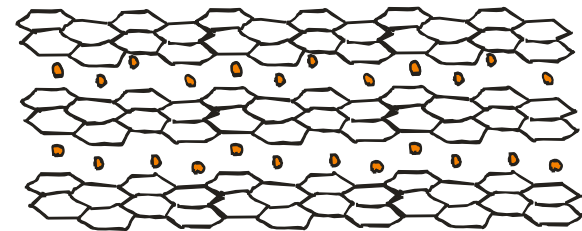
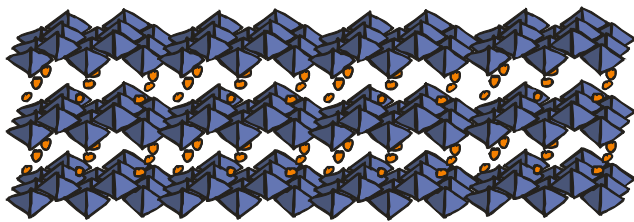


$\text{LiMn}_2\text{O}_4$   
 $\text{LiCoO}_2$   
 $(\text{Li})\text{FePO}_4$   
 $(\text{Li})\text{V}_2\text{O}_5$

$\text{Li}_2\text{CO}_3$   
 $\text{Li(OH)}$   
 $\text{Li-La-O}$   
 $\text{Li}_{0.32}\text{La}_{0.30}\text{TiO}_z$   
 $\text{LiAlO}_2$   
 $\text{Li}_x\text{SiO}_y$   
 $\text{Li}_x\text{Al}_z\text{SiO}_y$   
 $\text{LiNbO}_3$   
 $\text{LiTaO}_3$   
 $\text{Li}_3\text{PO}_4$   
 $\text{LiPON}$   
 $\text{LiF}$   
 $\text{Li}_3\text{N}$

$\text{Li}_x\text{TiO}_y$   
 $\text{TiO}_2$

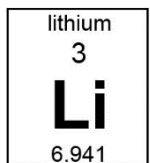
# Li-film battery



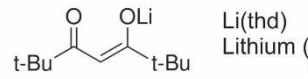
$\text{LiMn}_2\text{O}_4$   
 $\text{LiCoO}_2$   
 $(\text{Li})\text{FePO}_4$   
 $(\text{Li})\text{V}_2\text{O}_5$

$\text{Li}_2\text{CO}_3$   
 $\text{Li}(\text{OH})$   
 $\text{Li-La-O}$   
 $\text{Li}_{0.32}\text{La}_{0.30}\text{TiO}_z$   
 $\text{LiAlO}_2$   
 $\text{Li}_x\text{SiO}_y$   
 $\text{Li}_x\text{Al}_z\text{SiO}_y$   
 $\text{LiNbO}_3$   
 $\text{LiTaO}_3$   
 $\text{Li}_3\text{PO}_4$   
 $\text{LiPON}$   
 $\text{LiF}$   
 $\text{Li}_3\text{N}$

$\text{Li}_x\text{TiO}_y$   
 $\text{TiO}_2$



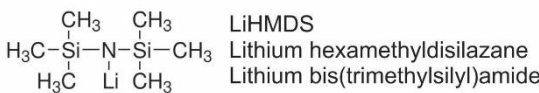
# - precursors



$\text{Li}(\text{thd})$   
Lithium (2,2,6,6-tetramethyl-3,5-heptanedionato)



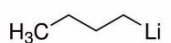
$\text{Li}(\text{'Bu})$   
Lithium *tert*-butoxide



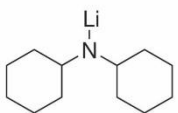
$\text{LiHMDS}$   
Lithium hexamethyldisilazane  
Lithium bis(trimethylsilyl)amide



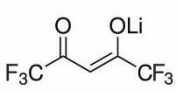
$\text{Li}(\text{Cp})$   
Cyclopentadienyllithium



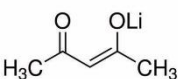
BuLi  
Butyllithium



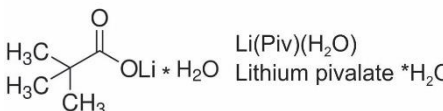
Lithium dicyclohexylamide



$\text{Li}(\text{hfac})$   
Lithium(1,1,1,5,5-hexafluoro-2,4-pentanedionato)  
Lithium hexafluoroacetylacetone



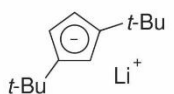
$\text{Li}(\text{acac})$   
Lithium acetylacetone



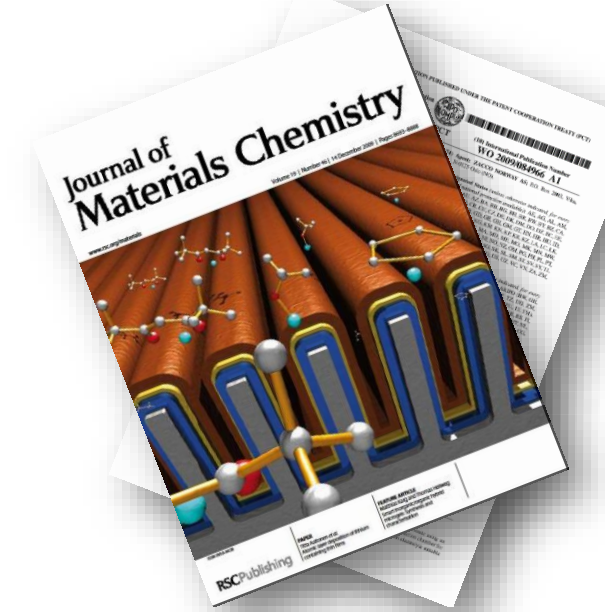
$\text{Li}(\text{Piv})(\text{H}_2\text{O})$   
Lithium pivalate \* $\text{H}_2\text{O}$



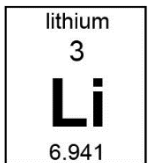
$\text{Li}(\text{CH}_3\text{SiMe}_3)$   
Lithium trimethylsilane



$\text{Li}(\text{'Bu}2\text{Cp})$   
Lithium Di-*tert*-butylcyclopentadiene

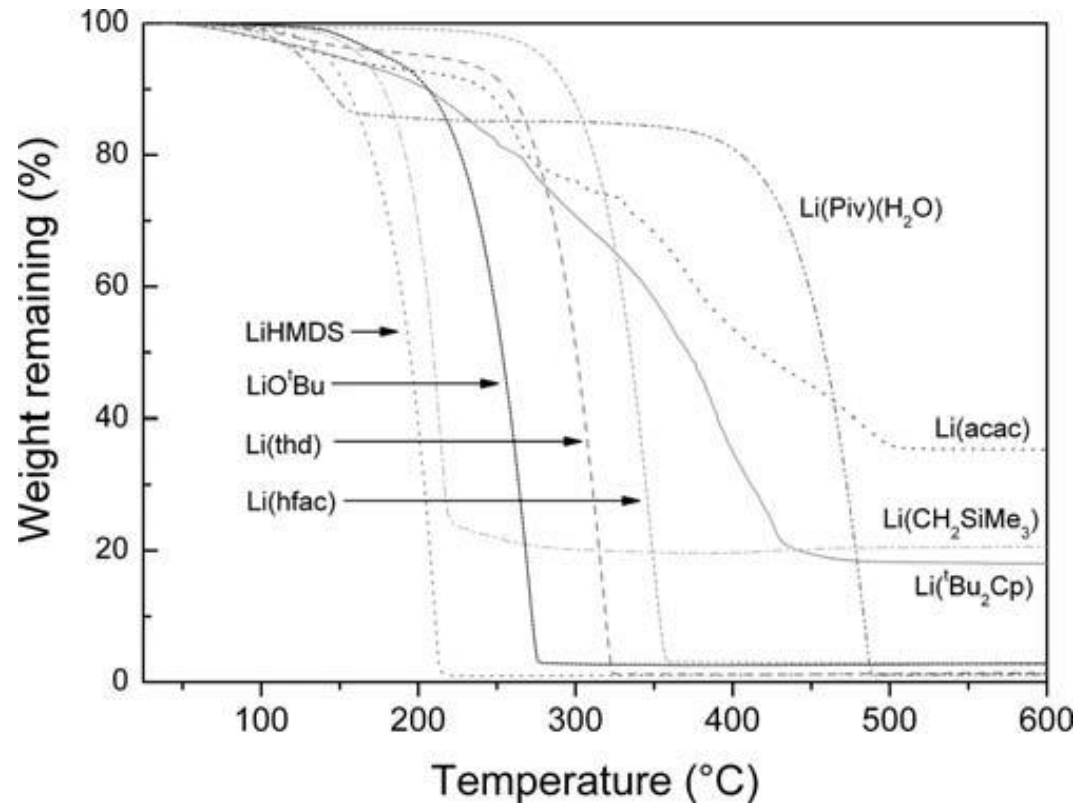


M. Putkonen, T. Aaltonen, M. Alnes, T. Sajavaara, O. Nilsen, and H. Fjellvåg, *J. Mater. Chem.* **19**, 8767 (2009).



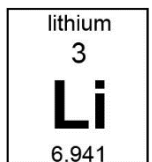
# - precursors

	<chem>CC(C)(C)C[C@H](O)C</chem>	<chem>Li(O'Bu)</chem> Lithium <i>tert</i> -butoxide
	<chem>CC(C)(C)Si(C)(C)N(C)C</chem>	<chem>LiHMDS</chem> Lithium hexamethyldisilazane Lithium bis(trimethylsilyl)amide
	<chem>C1=CC=C1</chem>	<chem>Li(Cp)</chem> Cyclopentadienyllithium
	<chem>CC(C)CCCLi</chem>	<chem>BuLi</chem> Butyllithium
	<chem>C1CCCCN(C)C1</chem>	Lithium dicyclohexylamide
	<chem>CC(F)(F)C(=O)C=C(C(F)(F)C(=O)C)C(F)(F)C</chem>	<chem>Li(hfac)</chem> Lithium(1,1,1,5,5-hexafluoro-2,4-pantanediato) Lithium hexafluoroacetylacetone
	<chem>CC(=O)C=C(C(=O)C)C</chem>	<chem>Li(acac)</chem> Lithium acetylacetoneate
	<chem>CC(C)(C)C[C@H](O)C(=O)C</chem>	<chem>Li(Piv)(H2O)</chem> Lithium pivalate *H <sub>2</sub> O
	<chem>CC(C)(C)C[C@H](O)Si(C)(C)C</chem>	<chem>Li(CH3SiMe3)</chem> Lithium trimethylsilane
	<chem>C1=CC=C1</chem>	<chem>Li('Bu2Cp)</chem> Lithium Di- <i>tert</i> -butylcyclopentadiene

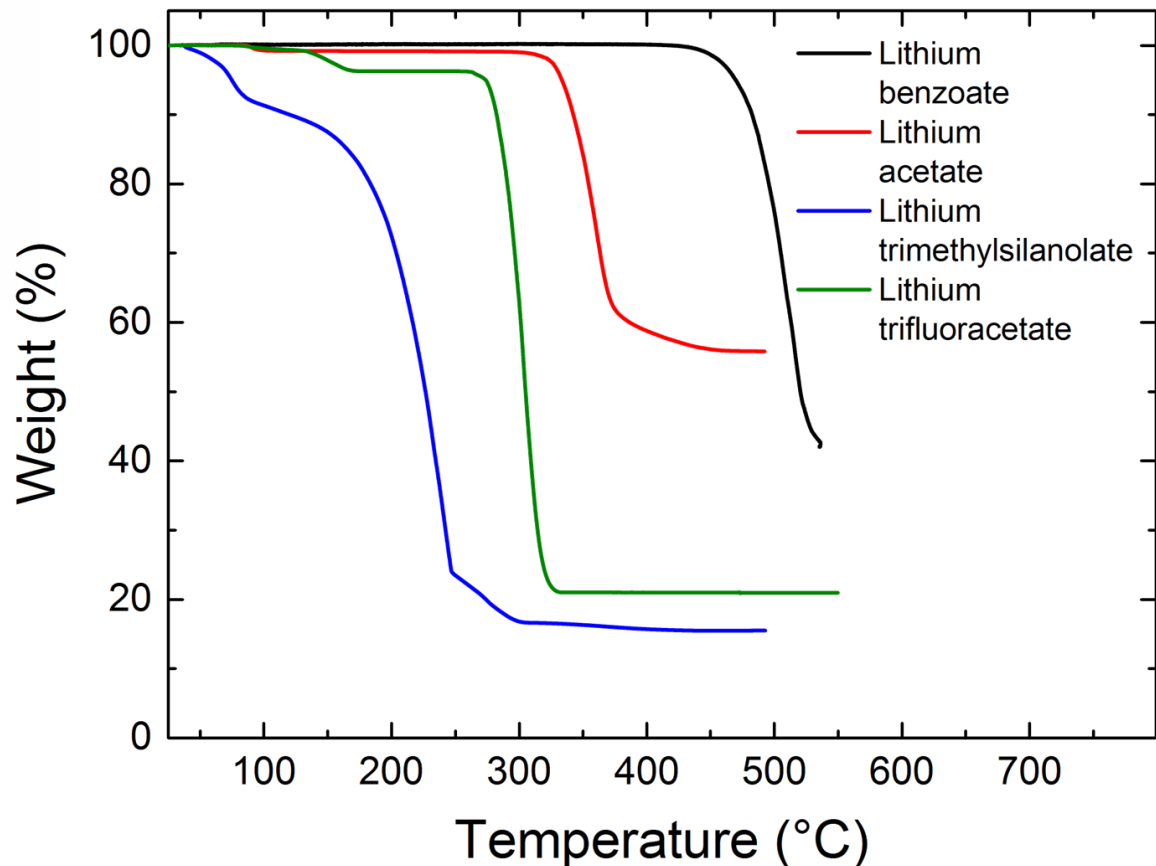
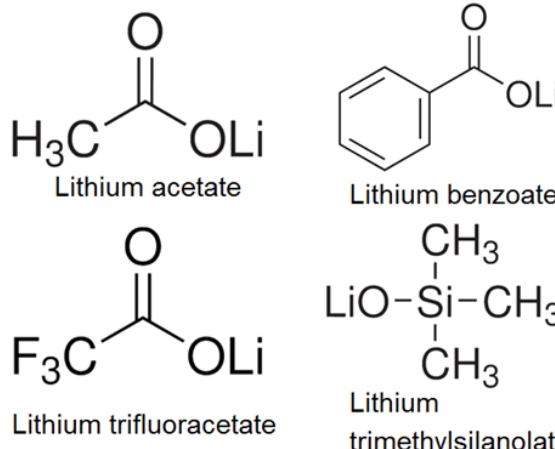
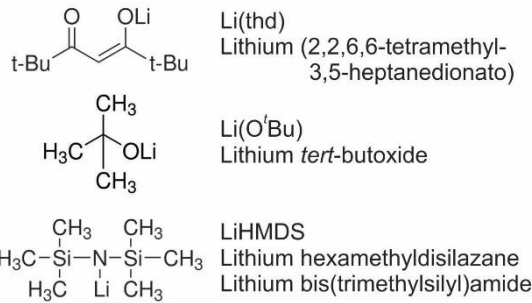


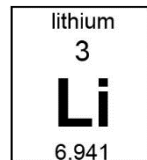
J. Hamalainen, J. Holopainen, F. Munnik, T. Hatanpaa, M. Heikkila, M. Ritala, and M. Leskela, *J. Electrochem. Soc.* **159**, A259 (2012).

M. Putkonen, T. Aaltonen, M. Alnes, T. Sajavaara, O. Nilsen, and H. Fjellvåg, *J. Mater. Chem.* **19**, 8767 (2009).



## - precursors

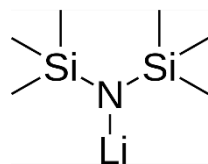




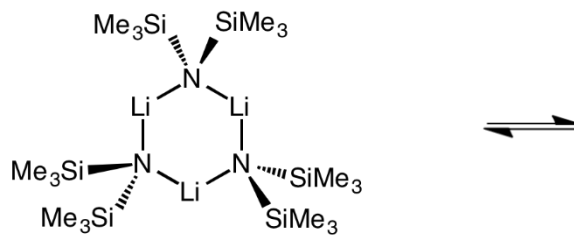
# Why is Li not straight forward?

Monovalent, ...so are Cu(I)Cl, Ag<sup>+</sup>, In(I)Cl...

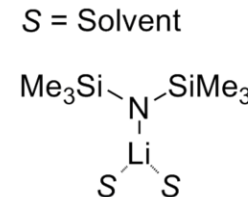
⇒ As monomer, what terminates the surface?



Does not exist



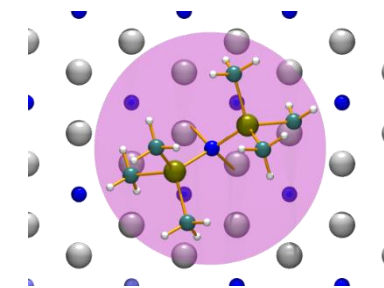
Sublimes as trimer

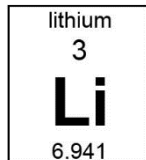


Monomer and dimer in solvated form



Ref. to growth of Li<sub>3</sub>N later...





# Why is Li not straight forward?

Monovalent, ...so are Cu(I)Cl, Ag<sup>+</sup>, In(I)Cl...

⇒ As monomer, what terminates the surface?

Basic oxide?

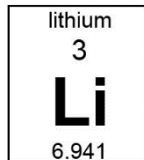
⇒ Basic oxides tend to absorb water and CO<sub>2</sub>...



Ref. to growth of Li<sub>2</sub>CO<sub>3</sub> later...

Same for growth of Na and K compounds?

Yes...



# Why is Li not straight forward?

Monovalent, ...so are Cu(I)Cl, Ag<sup>+</sup>, In(I)Cl...

⇒ As monomer, what terminates the surface?

Basic oxide?

⇒ Basic oxides tend to absorb water and CO<sub>2</sub>...

Mobile ions?

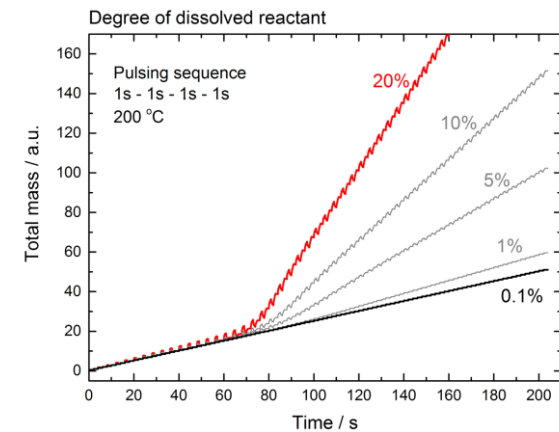
⇒ The aim is Li-ion conducting materials..., after all...

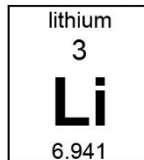


Ref. to growth of LiAlO<sub>2</sub> later...

⇒ Reservoir growth

Ref. to lithiation of MnO<sub>2</sub> and V<sub>2</sub>O<sub>5</sub>





# Why is Li not straight forward?

Monovalent, ...so are Cu(I)Cl, Ag<sup>+</sup>, In(I)Cl...

⇒ As monomer, what terminates the surface?

Basic oxide?

⇒ Basic oxides tend to absorb water and CO<sub>2</sub>...

Mobile ions?

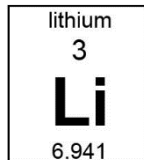
⇒ The aim is Li-ion conducting materials..., after all...

Control composition?

⇒ A sum of the above...



Need a good selection of precursor chemistries



# Why is Li not straight forward?

Monovalent, ...so are Cu(I)Cl, Ag<sup>+</sup>, In(I)Cl...

⇒ As monomer, what terminates the surface?

Basic oxide?

⇒ Basic oxides tend to absorb water and CO<sub>2</sub>...

Mobile ions?

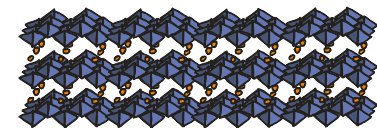
⇒ The aim is Li-ion conducting materials..., after all...

Control composition?

⇒ A sum of the above...

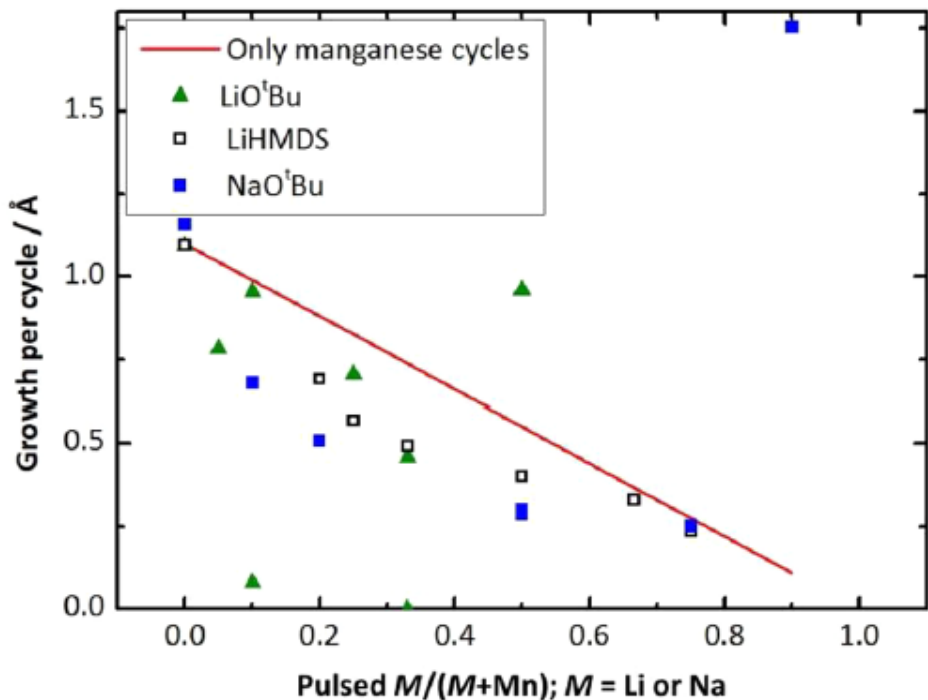
Freshness of precursor?

⇒ Batch differences...



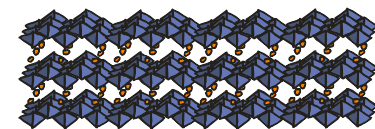
# $\text{LiMn}_2\text{O}_4$ using $[\text{LiOtBu} + \text{H}_2\text{O}] + [\text{Mn}(\text{EtCp})_2 + \text{H}_2\text{O}]$

The same result with  $[\text{Li}(\text{thd}) + \text{O}_3] + [\text{Mn}(\text{thd})_3 + \text{O}_3]$ ...



Almost no Li or Na incorporated into the film during growth

Figure 1. Film growth per cycle vs pulsing ratio (proportion of alkali-metal subcycles in a supercycle) using  $\text{Mn}(\text{EtCp})_2$  as the Mn precursor. The line represents the theoretical growth per cycle with no contribution from alkali-metal subcycles to the film growth.



# LiMn<sub>2</sub>O<sub>4</sub>

The same result with [Li(thd) + O<sub>3</sub>] + [Mn(thd)<sub>3</sub> + O<sub>3</sub>]...

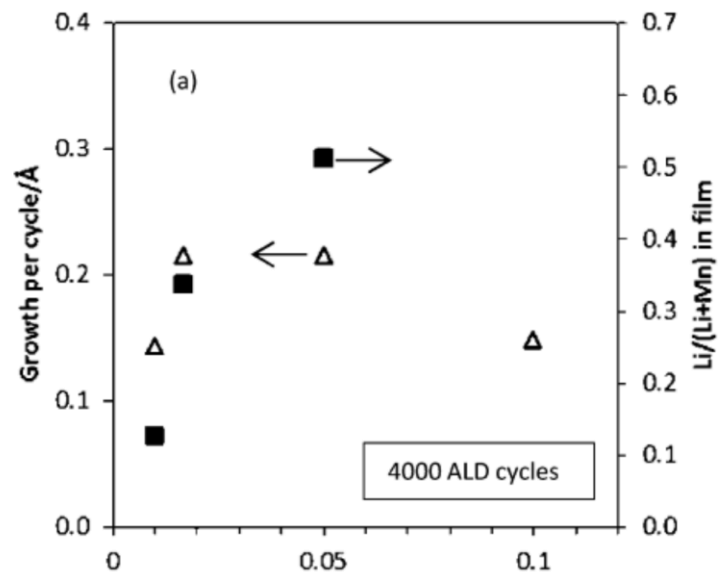


Figure 2. Growth per cycle and relative lithium composition for  $\text{Li}_x\text{Mn}_y\text{O}_z$  films deposited with Li(thd) as the lithium precursor for films with (a) 4000 and (b) 1000 deposition cycles.

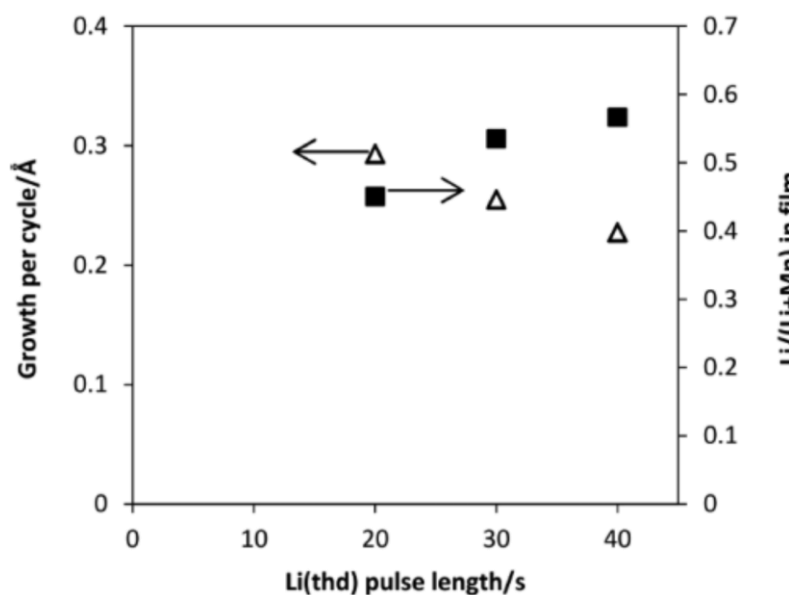
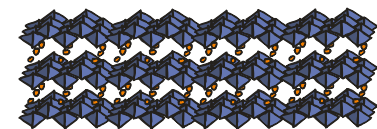


Figure 4. Film growth per cycle and relative lithium composition for  $\text{Li}_x\text{Mn}_2\text{O}_4$  films deposited with a pulsing sequence of  $100 \times \{19 \times [\text{Mn}(\text{thd})_3 (1.5/1) + \text{O}_3 (5/5)] + [\text{Li}(\text{thd}) (X/10) + \text{O}_3 (5/5)\}\}$ .

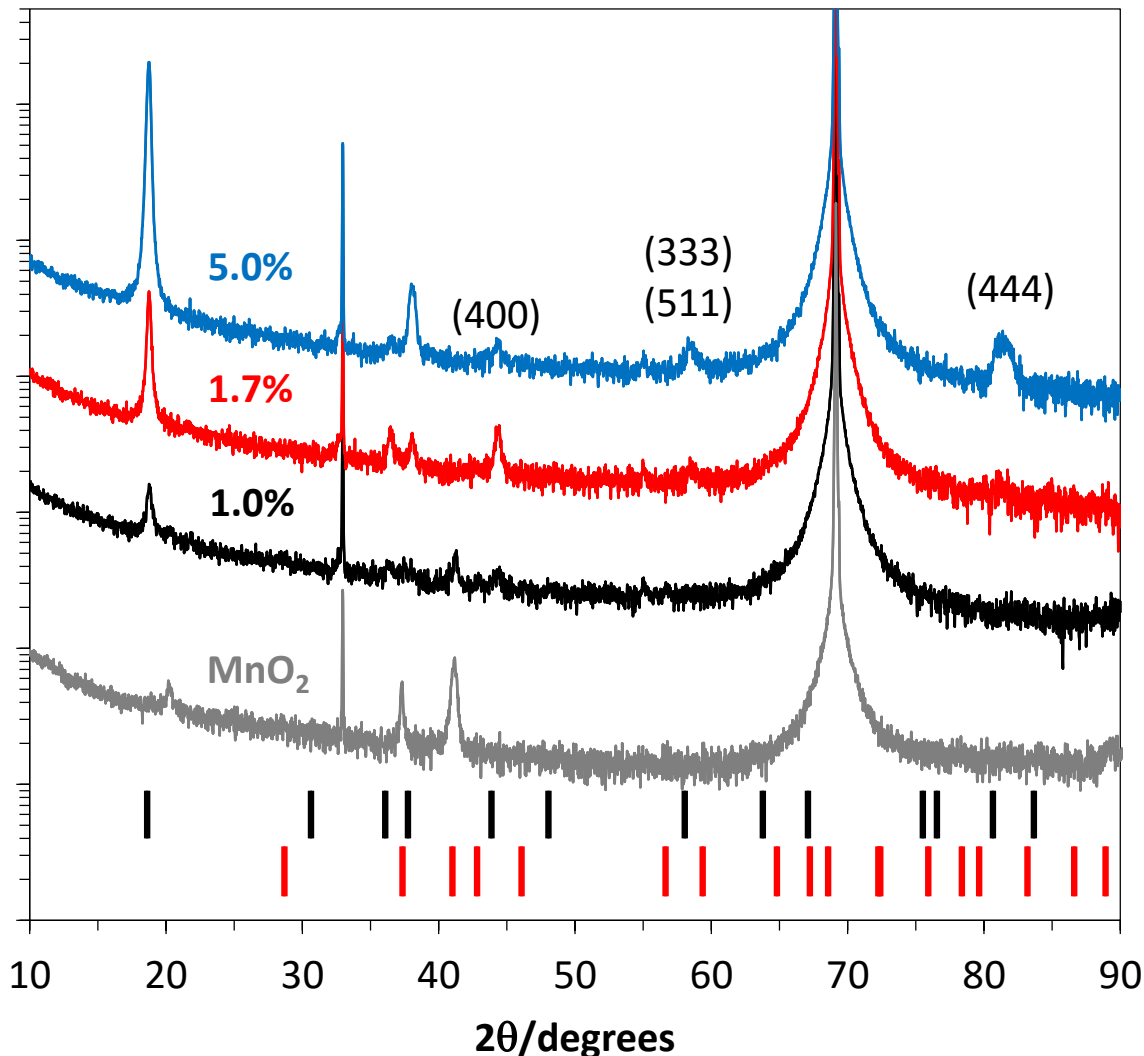


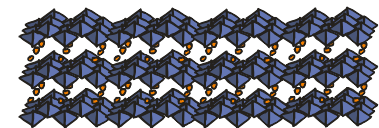
# LiMn<sub>2</sub>O<sub>4</sub>

The same result with [Li(thd) + O<sub>3</sub>] + [Mn(thd)<sub>3</sub> + O<sub>3</sub>]...

## XRD for 4000-cycle films on Si(100):

- Spinel  $\text{Li}_x\text{Mn}_2\text{O}_4$  | visible throughout the series
- MnO<sub>2</sub> impurity | with 1.0% pulsed Li
- Film with 5.0% pulsed Li [111] oriented





## Gas phase lithiation

$[\text{Li}(\text{thd}) + \text{O}_3]$  = fixed composition

$[\text{LiO}^t\text{Bu} + \text{H}_2\text{O}]$  = fixed composition

...

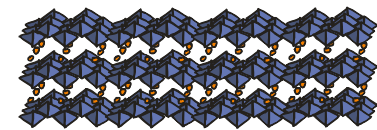
Grew films of:

$\text{V}_2\text{O}_5$ ,  $\text{MnO}_2$ ,  $\text{TiO}_2$ ,  $\text{Al}_2\text{O}_3$ ,  $\text{ZnO}$ ,  $\text{Co}_3\text{O}_4$ ,  $\text{Fe}_2\text{O}_3$ ,  $\text{NiO}$

Tried lithiation using  $[\text{Li}(\text{thd}) + \text{O}_3]$  or  $[\text{LiO}^t\text{Bu} + \text{H}_2\text{O}]$

Got: unaltered films for  $\text{TiO}_2$ ,  $\text{Al}_2\text{O}_3$ ,  $\text{ZnO}$ ,  $\text{Co}_3\text{O}_4$ ,  $\text{Fe}_2\text{O}_3$ ,  $\text{NiO}$

->  $\text{V}_2\text{O}_5$ ,  $\text{MnO}_2$  ?



# Gas phase lithiation: $\text{MnO}_2$

$[\text{Li}(\text{thd}) + \text{O}_3]$  = fixed composition

$[\text{LiO}^t\text{Bu} + \text{H}_2\text{O}]$  = fixed composition

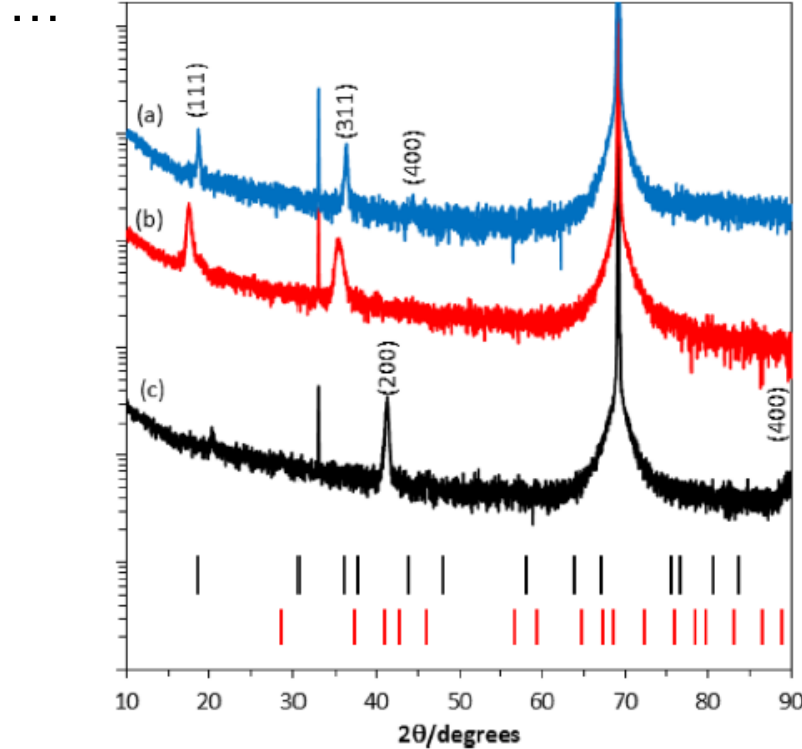
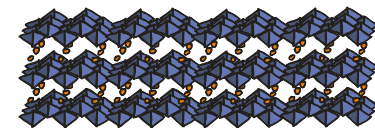


Figure 6. XRD diffractograms of (a)  $\text{Li}(\text{thd})-\text{O}_3$ -treated (100 ALD cycles) and annealed  $\text{MnO}_2$ , (b)  $\text{Li}(\text{thd})-\text{O}_3$ -treated  $\text{MnO}_2$ , and (c) as-deposited  $\text{MnO}_2$  (110 nm). Films were deposited on Si(100). Black and red tick marks below the graphs refer to  $\text{LiMn}_2\text{O}_4$  spinel (35-0782) and pyrolusite  $\beta\text{-MnO}_2$  (24-0735), respectively.

As lithiated and annealed:  $\text{LiMn}_2\text{O}_4$

As lithiated:  $\text{LiMn}_2\text{O}_4$

Started with:  $\text{MnO}_2$



# Gas phase lithiation: $\text{MnO}_2$

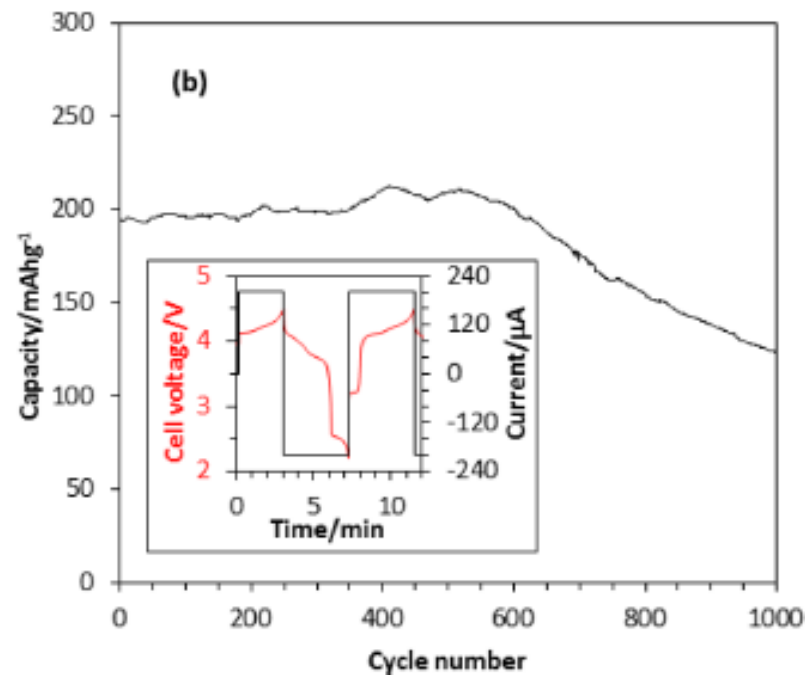
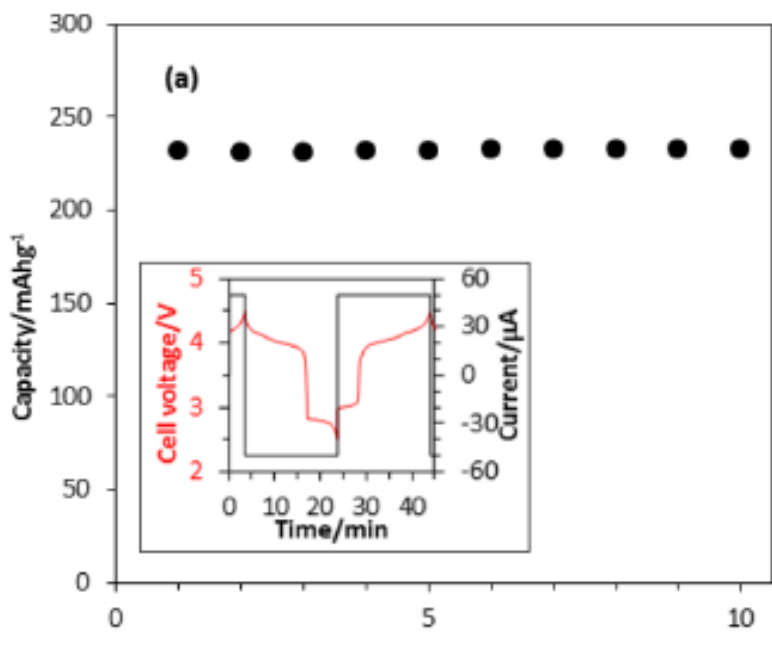
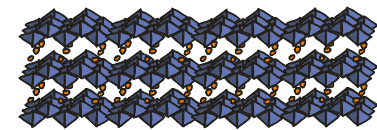


Figure 11. Discharge capacities and first-cycle potentiograms (insets) of an 86-nm  $\text{MnO}_2$  film treated with 200 cycles of  $\text{LiO}^\bullet\text{Bu} + \text{H}_2\text{O}$ : (a) 10 charge–discharge cycles with 50  $\mu\text{A}$ , (b) 1000 charge–discharge cycles with 200  $\mu\text{A}$ .



# Gas phase lithiation: $\text{V}_2\text{O}_5$

$[\text{Li}(\text{thd}) + \text{O}_3]$  = fixed composition

$[\text{LiO}^t\text{Bu} + \text{H}_2\text{O}]$  = fixed composition

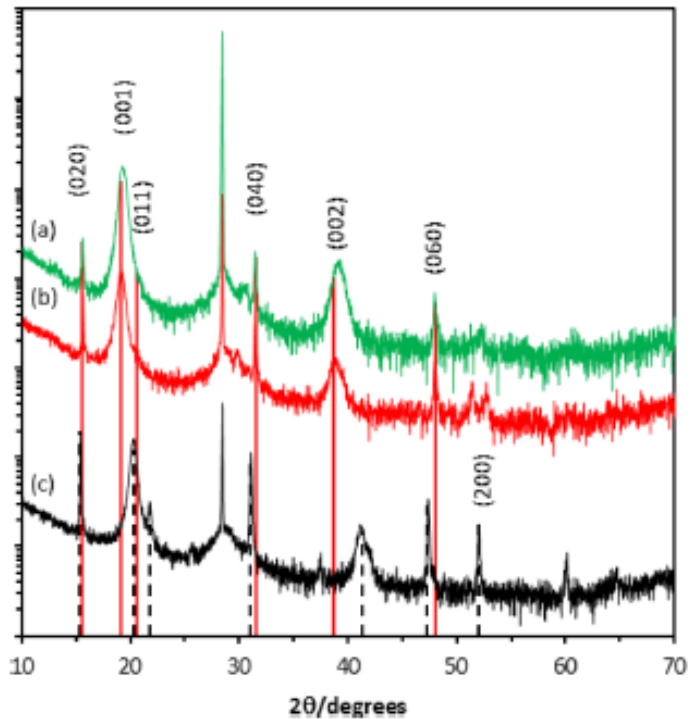


**Figure 8.** XRD diffractograms of (a)  $\text{Li}_x\text{V}_2\text{O}_5$  films made with  $\text{LiO}^t\text{Bu}-\text{H}_2\text{O}$  treatment, (b)  $\text{Li}_x\text{V}_2\text{O}_5$  films made with  $\text{Li}(\text{thd})-\text{O}_3$  treatment, and (c) parent  $\text{V}_2\text{O}_5$  film on  $\text{Si}(111)$ . Indexing refers to the  $Pmmn$  space group for  $\text{V}_2\text{O}_5$  and  $\varepsilon\text{-Li}_x\text{V}_2\text{O}_5$ <sup>35</sup> with unit cell dimensions of  $a = 3.57 \text{ \AA}$ ,  $b = 11.54 \text{ \AA}$ ,  $c = 4.38 \text{ \AA}$  and  $a = 3.57 \text{ \AA}$ ,  $b = 11.36 \text{ \AA}$ ,  $c = 4.65 \text{ \AA}$ , respectively. Dashed black lines and red lines refer to  $\alpha\text{-V}_2\text{O}_5$  and  $\varepsilon\text{-Li}_x\text{V}_2\text{O}_5$ , respectively.

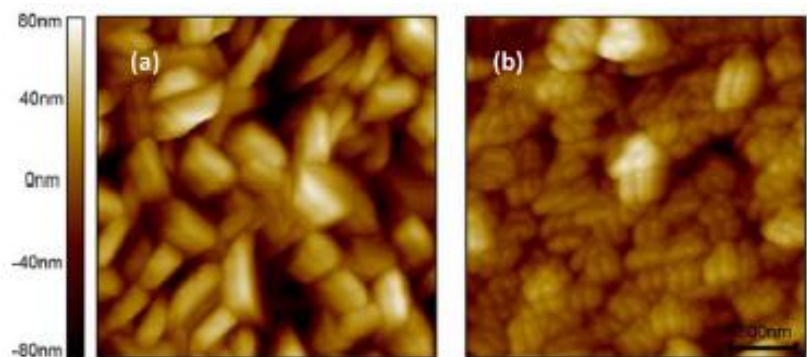
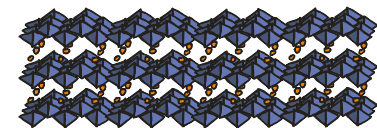


**Figure 9.** AFM images of (a)  $\text{V}_2\text{O}_5$  film and (b)  $\text{V}_2\text{O}_5$  film treated with 100 cycles of  $\text{LiO}^t\text{Bu} + \text{H}_2\text{O}$ .

As  $\text{LiO}^t\text{Bu}$  lithiated:  $\varepsilon\text{-Li}_x\text{V}_2\text{O}_5$

As  $\text{Li}(\text{thd})$  lithiated:  $\varepsilon\text{-Li}_x\text{V}_2\text{O}_5$

Started with:  $\alpha\text{-V}_2\text{O}_5$



# V<sub>2</sub>O<sub>5</sub>



J.C. Badot, ..., D. Lincotb, *Electrochem. Solid-State Lett.* **3** (2000) 485.



X. Chen, ..., G. Rubloff, *Chem.Mater.* **24** (2012) 1255.

O<sub>3</sub>-based ALD of crystalline V<sub>2</sub>O<sub>5</sub> cathodes

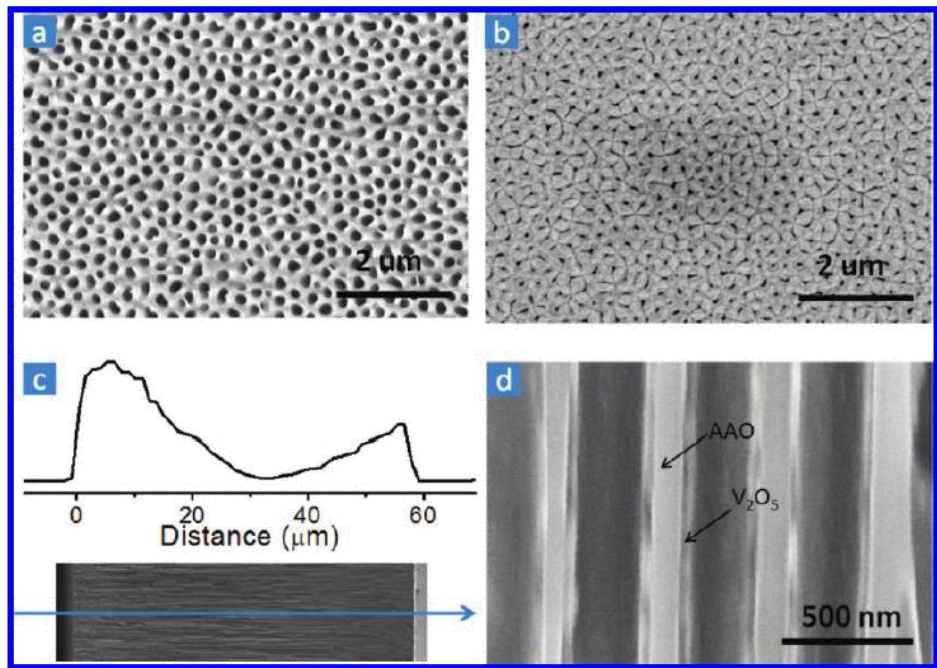
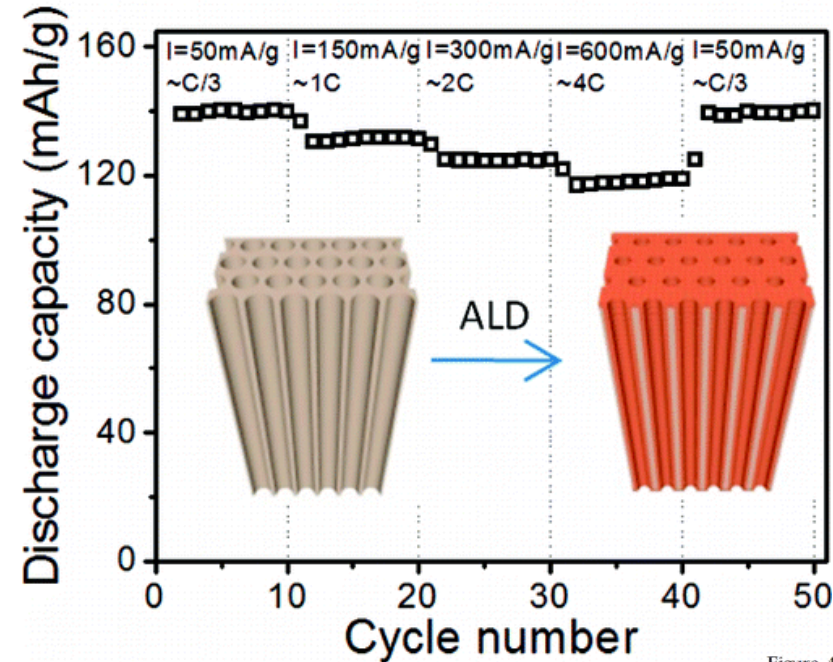
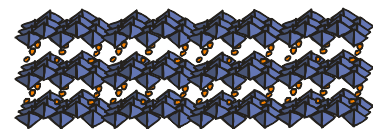


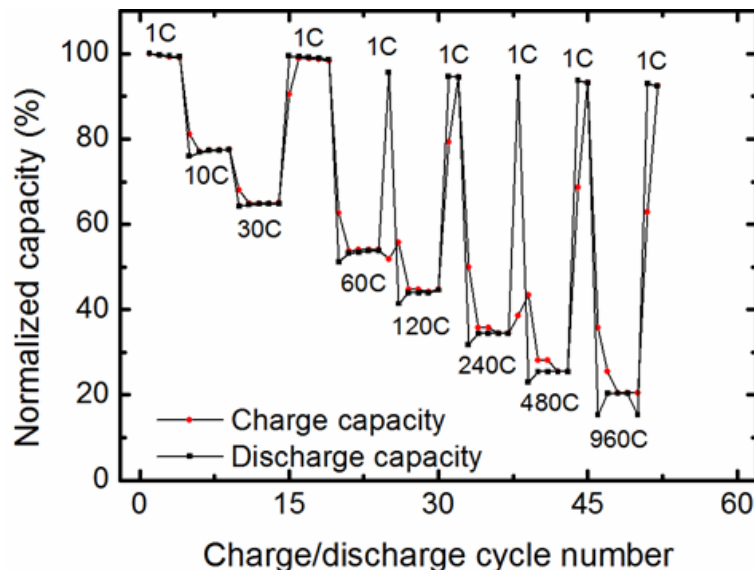
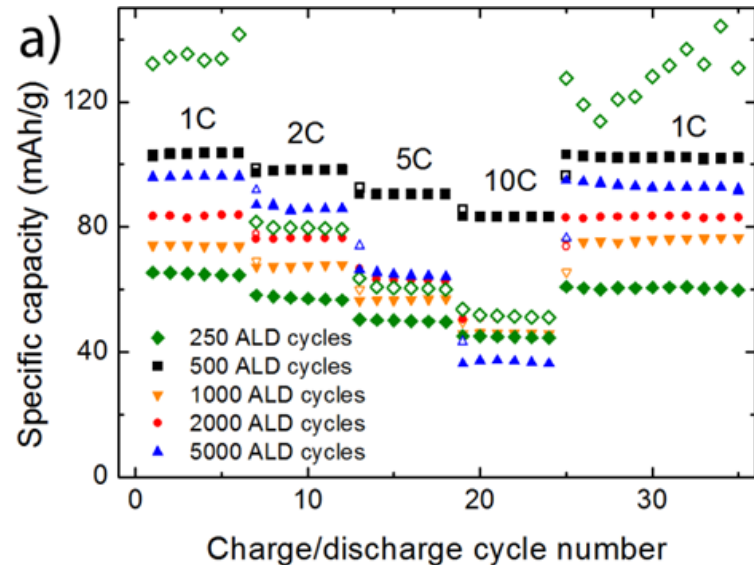
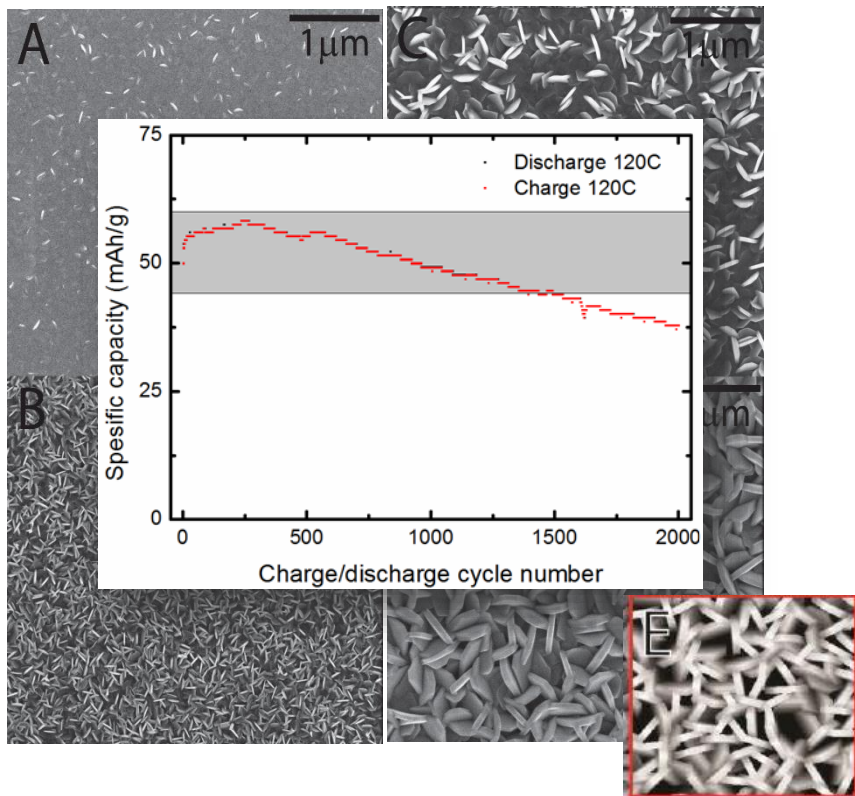
Figure 4. SEM of the AAO template (a) before and (b) after 1000 cycle ozone-based ALD V<sub>2</sub>O<sub>5</sub> film deposition; (c) EDX line scan of V signal through the cross-section of V<sub>2</sub>O<sub>5</sub> coated AAO template; (d) SEM image of V<sub>2</sub>O<sub>5</sub> nanotubes inside AAO pores.



# V<sub>2</sub>O<sub>5</sub>

V<sub>2</sub>O<sub>5</sub>    VO(thd)<sub>3</sub> + O<sub>3</sub>

E. Østreng, ..., H. Fjellvåg,  
*J. Mater. Chem. A*, **2** (2014) 15044

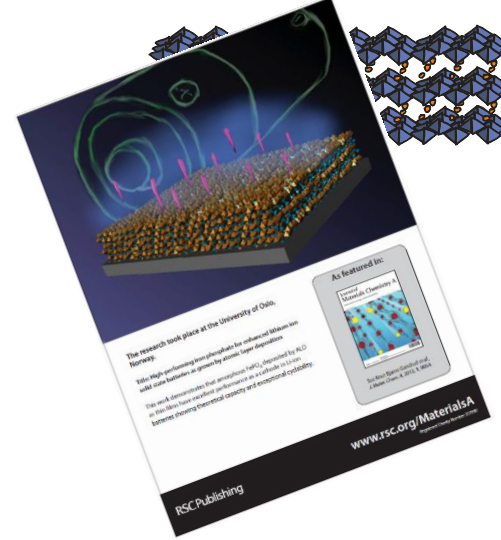
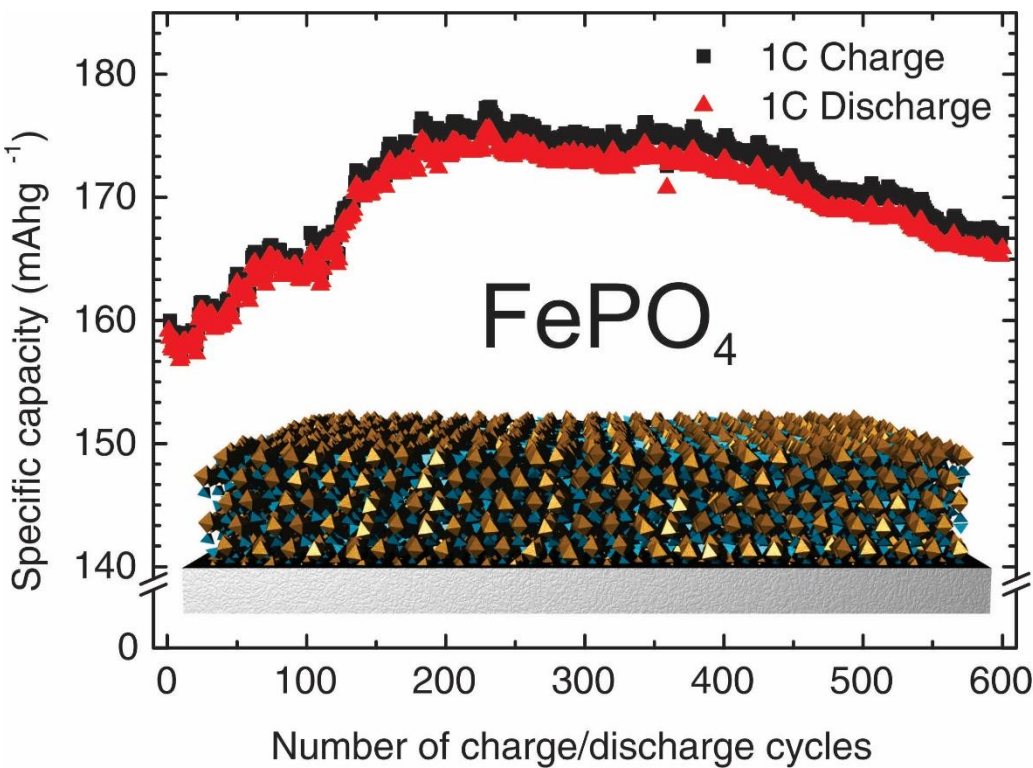
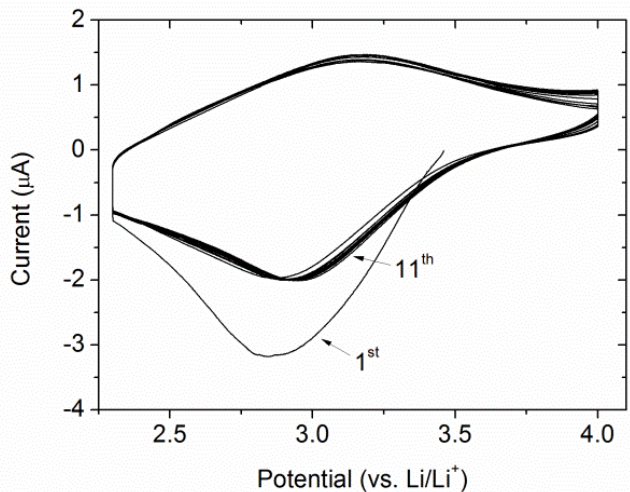
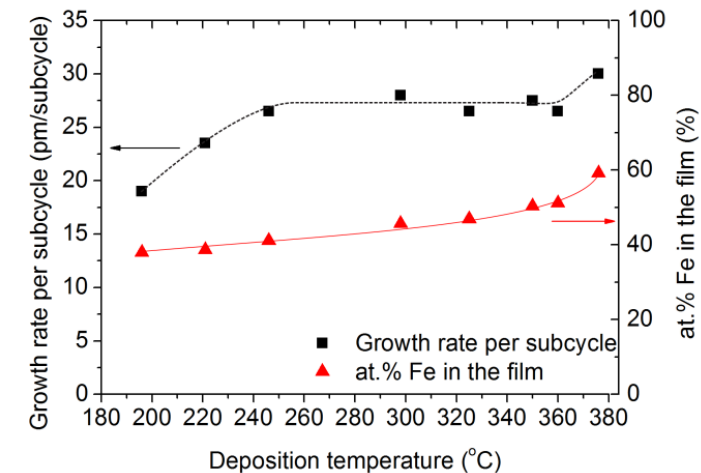


# FePO<sub>4</sub>

FePO<sub>4</sub>

Fe(thd)<sub>3</sub>/O<sub>3</sub> + Me<sub>3</sub>PO<sub>4</sub>/(H<sub>2</sub>O + O<sub>3</sub>)

K.B. Gandrud, ..., H. Fjellvåg, *J. Mater. Chem A* 1 (2013) 9054

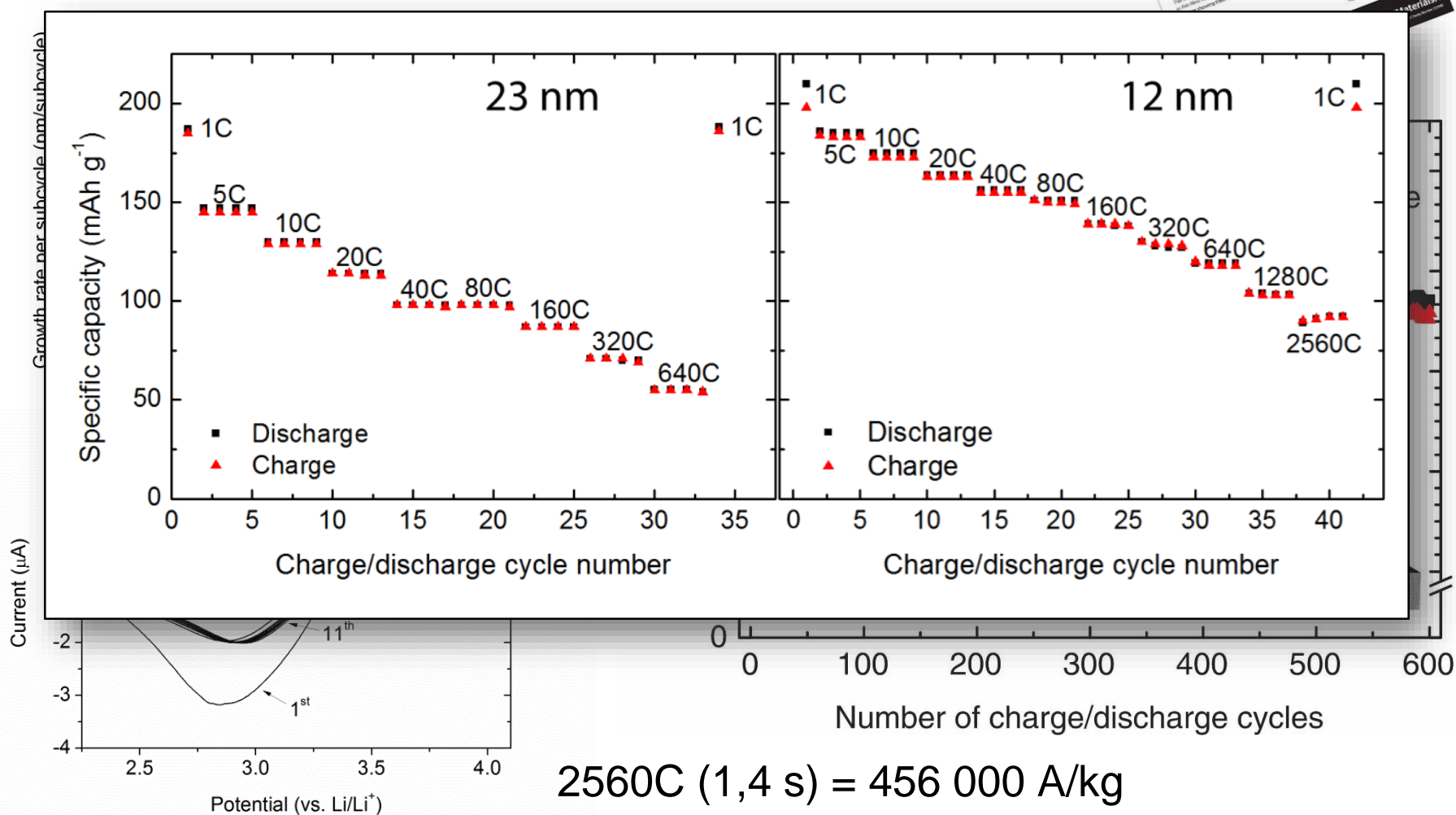
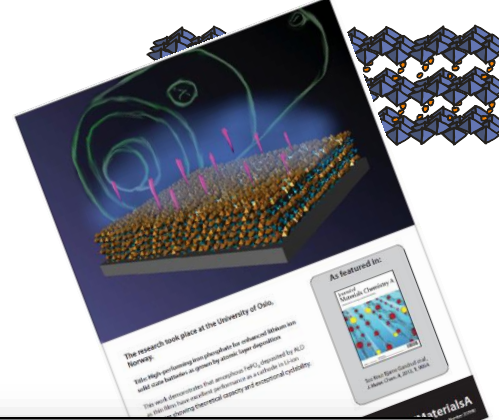


# FePO<sub>4</sub>

FePO<sub>4</sub>

Fe(thd)<sub>3</sub>/O<sub>3</sub> + Me<sub>3</sub>PO<sub>4</sub>/(H<sub>2</sub>O + O<sub>3</sub>)

K.B. Gandrud, ..., H. Fjellvåg, *J. Mater. Chem A* 1 (2013) 9054

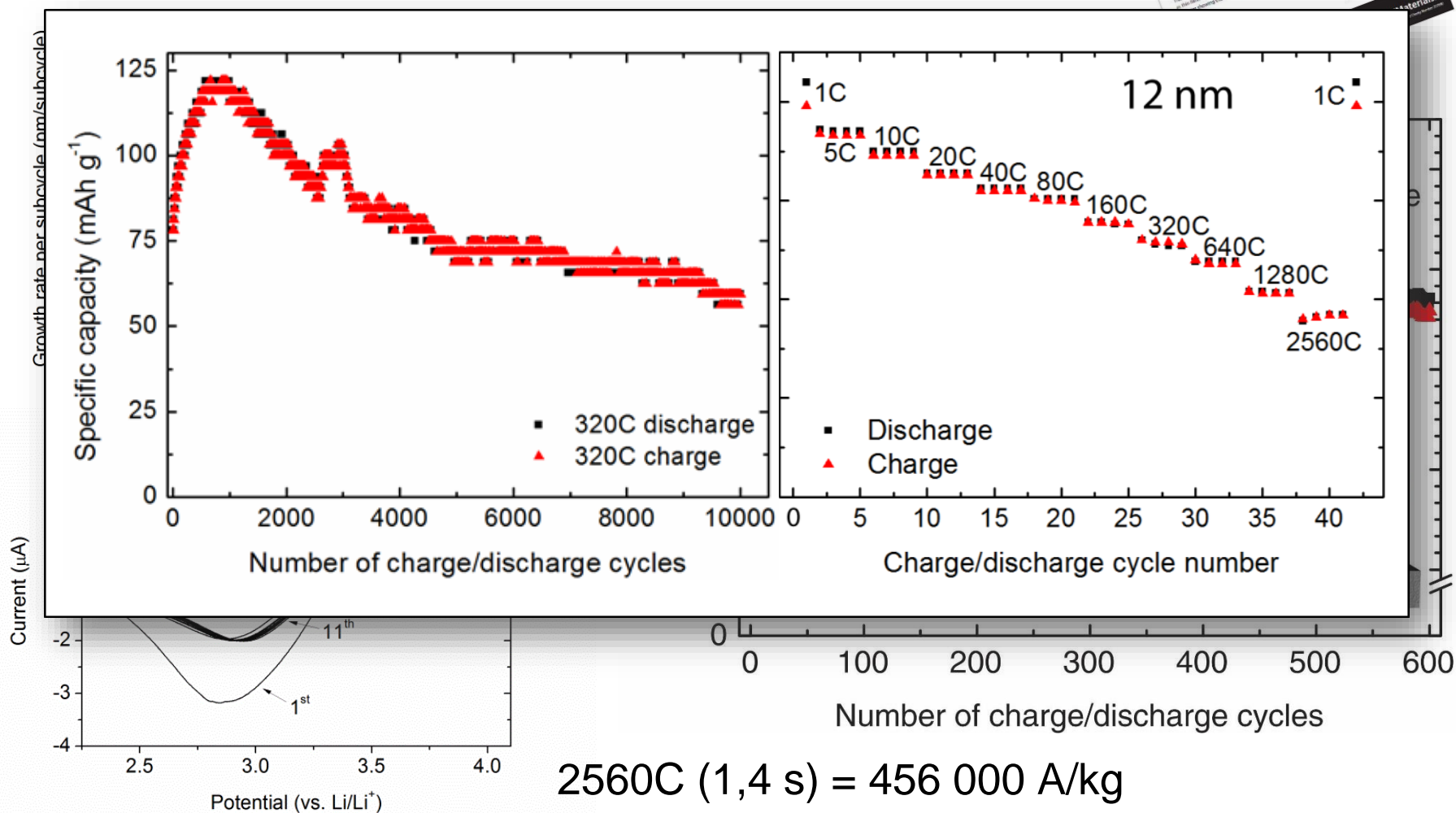
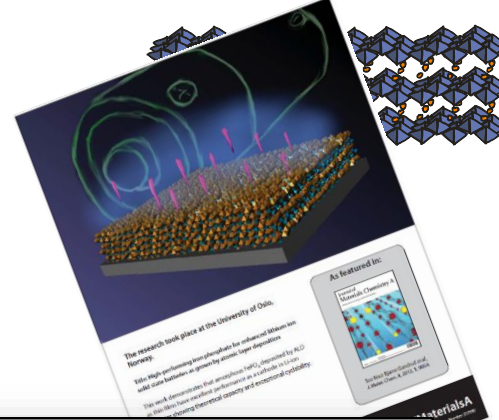


# FePO<sub>4</sub>

FePO<sub>4</sub>

Fe(thd)<sub>3</sub>/O<sub>3</sub> + Me<sub>3</sub>PO<sub>4</sub>/(H<sub>2</sub>O + O<sub>3</sub>)

K.B. Gandrud, ..., H. Fjellvåg, *J. Mater. Chem A* 1 (2013) 9054

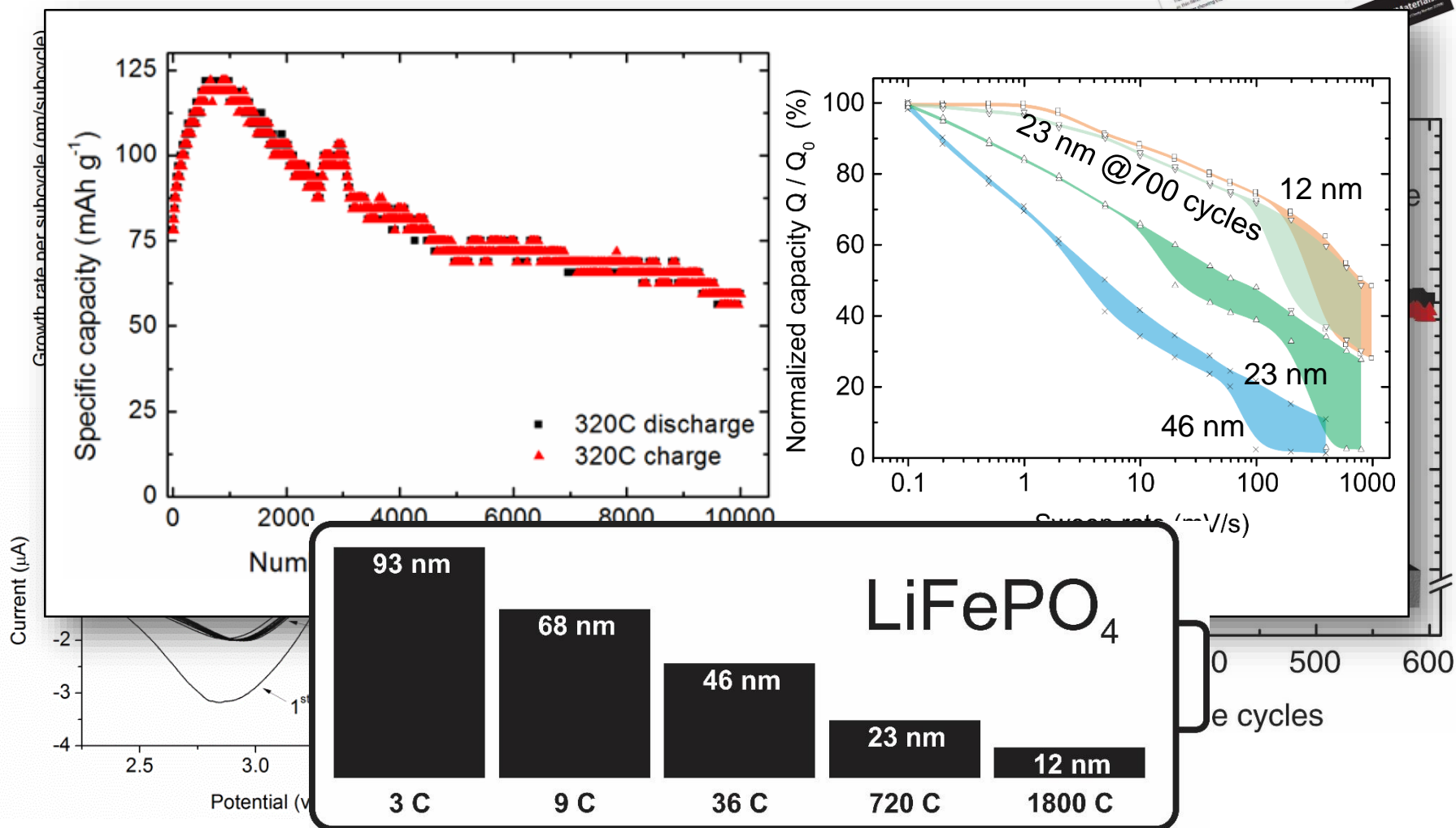
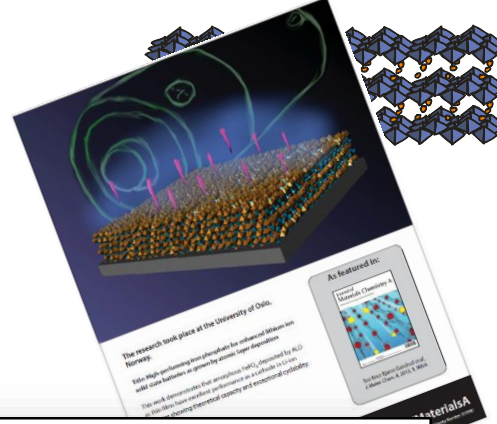


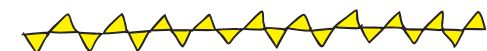
# FePO<sub>4</sub>

FePO<sub>4</sub>

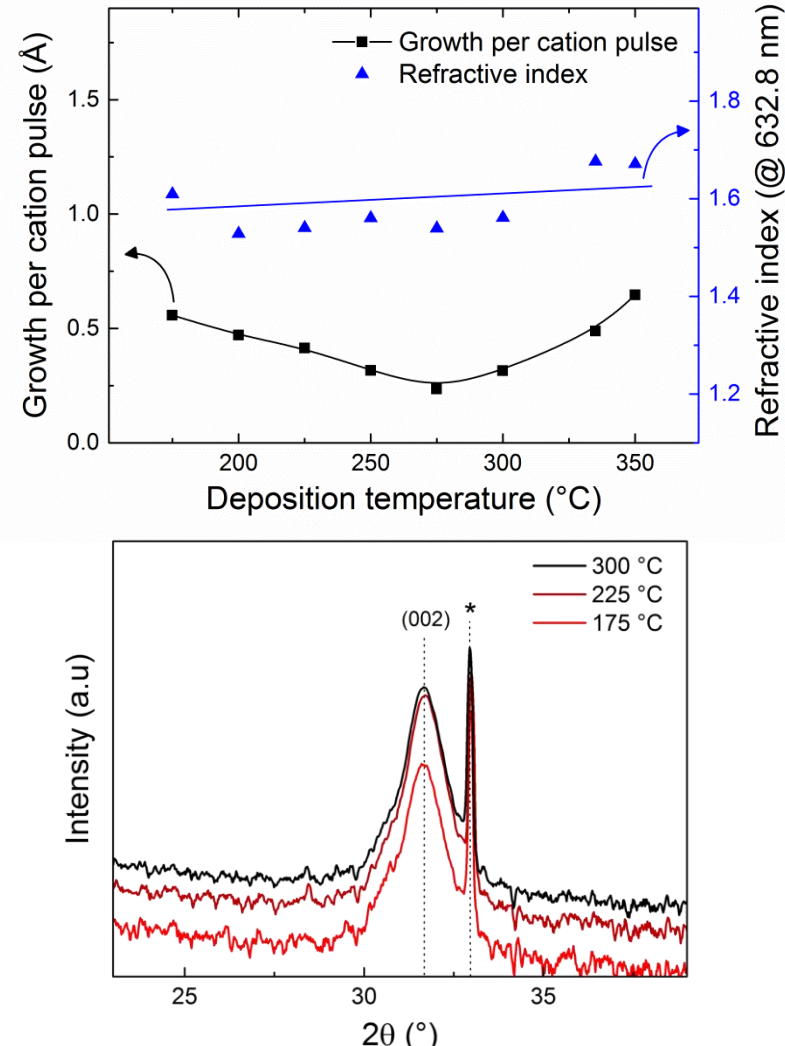
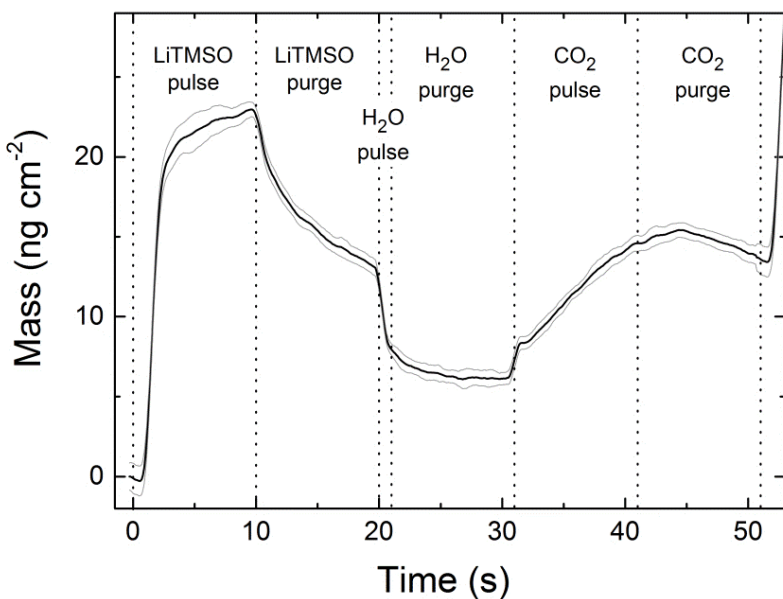
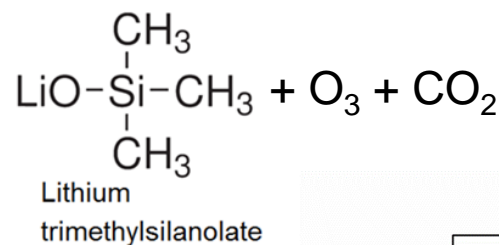
Fe(thd)<sub>3</sub>/O<sub>3</sub> + Me<sub>3</sub>PO<sub>4</sub>/(H<sub>2</sub>O + O<sub>3</sub>)

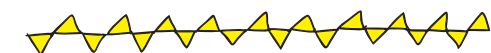
K.B. Gandrud, ..., H. Fjellvåg, *J. Mater. Chem A* 1 (2013) 9054





# $\text{Li}_2\text{CO}_3$



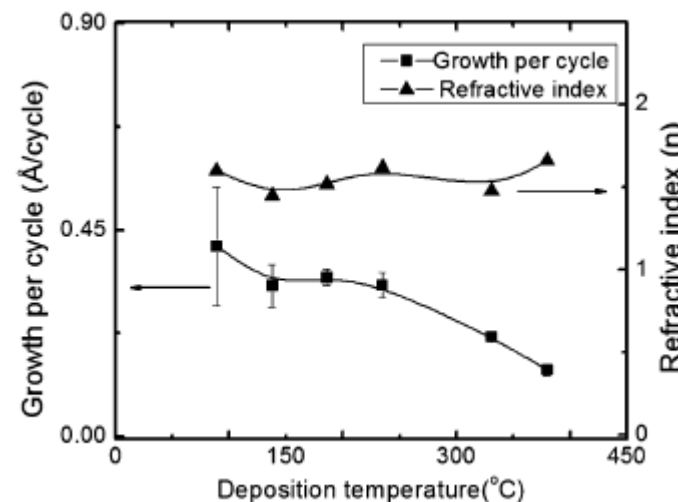
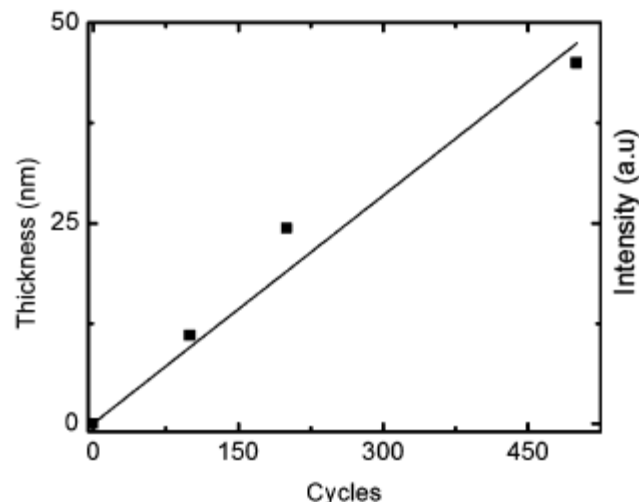
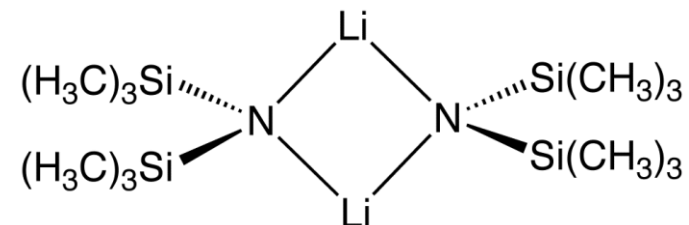


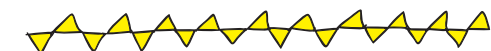
## LiHMDS ( $\text{Li(OH)}$ , $\text{Li}_2\text{CO}_3$ , $\text{Li}_3\text{N}$ )

$[\text{LiHMDS} + \text{H}_2\text{O}] = \text{reacts fast with air}$

$[\text{LiHMDS} + \text{NH}_3] = \text{reacts faster with air}$   
 - capped with  $\text{MoN}_x$

$[\text{LiHMDS} + \text{H}_2\text{O} + \text{CO}_2] = \text{Li}_2\text{CO}_3$



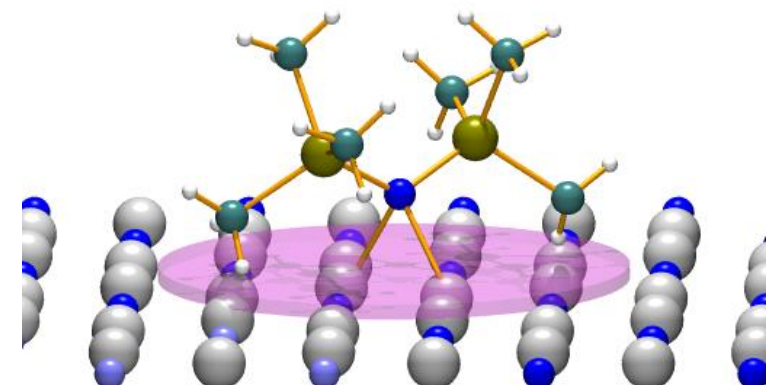
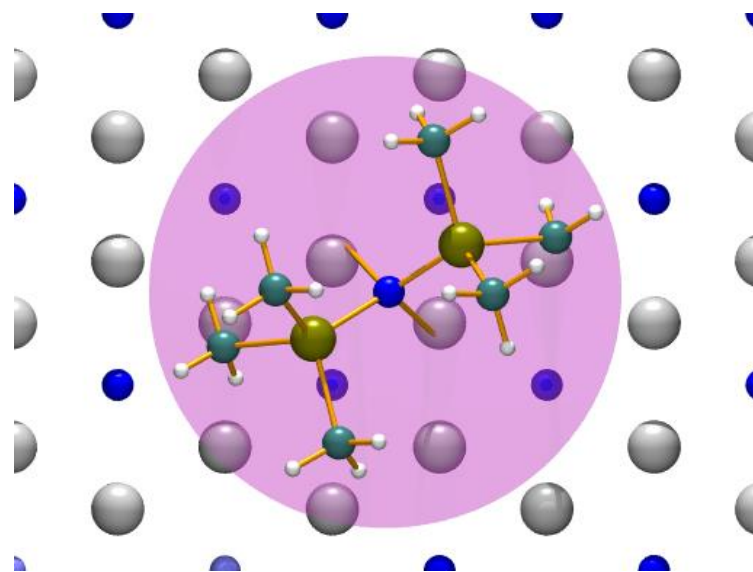
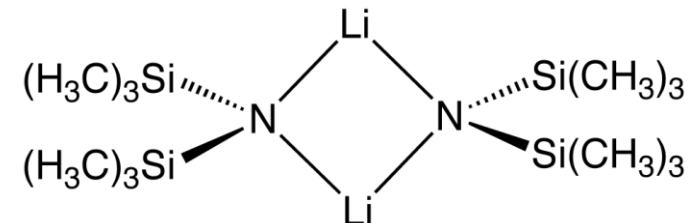


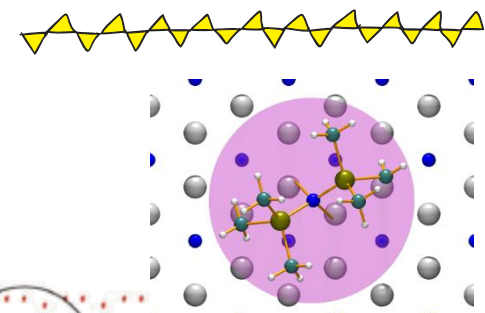
## LiHMDS ( $\text{Li(OH)}$ , $\text{Li}_2\text{CO}_3$ , $\text{Li}_3\text{N}$ )

$[\text{LiHMDS} + \text{H}_2\text{O}]$  = reacts fast with air

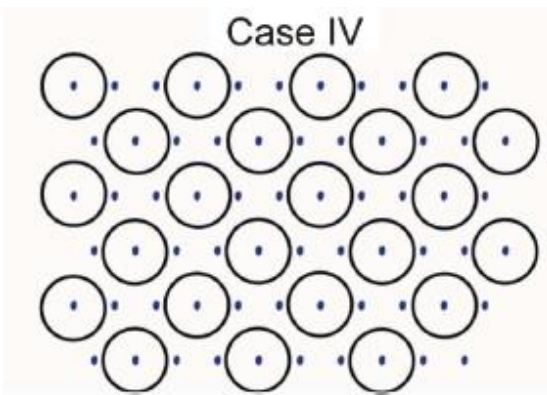
$[\text{LiHMDS} + \text{NH}_3]$  = reacts faster with air  
- capped with  $\text{MoN}_x$

$[\text{LiHMDS} + \text{H}_2\text{O} + \text{CO}_2]$  =  $\text{Li}_2\text{CO}_3$

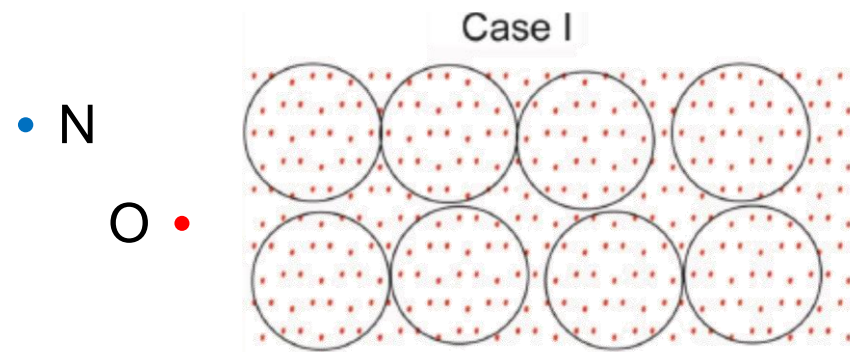




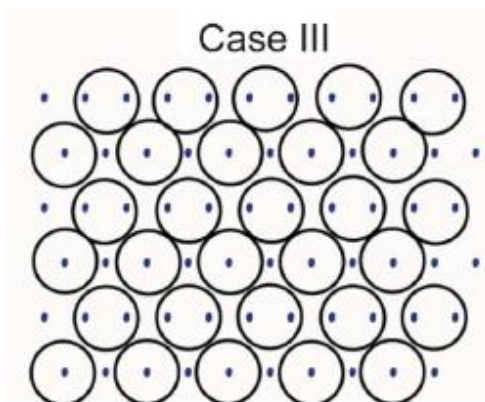
## LiHMDS ( $\text{Li}(\text{OH})$ , $\text{Li}_2\text{CO}_3$ , $\text{Li}_3\text{N}$ )



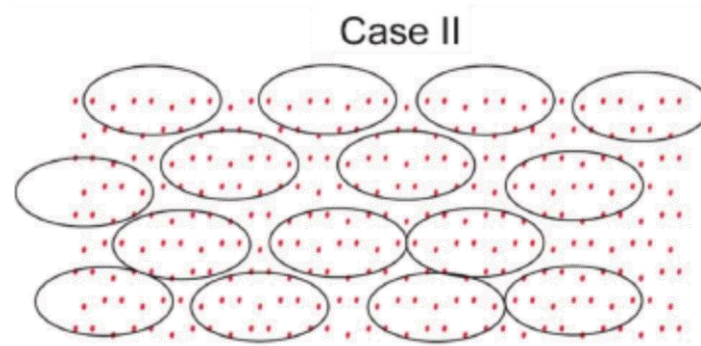
$$\text{GPC } (\text{Li}_3\text{N}) = 0.73 \text{ \AA/cycle}$$



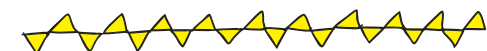
$$\text{GPC } (\text{Li}_2\text{CO}_3) = 0.23 \text{ \AA/cycle}$$
$$\text{GPC@331 } ^\circ\text{C} = 0.23 \text{ \AA/cycle}$$



$$\text{GPC } (\text{Li}_3\text{N}) = 1.1 \text{ \AA/cycle}$$
$$\text{GPC@167 } ^\circ\text{C} = 1.1 \text{ \AA/cycle}$$



$$\text{GPC } (\text{Li}_2\text{CO}_3) = 0.42 \text{ \AA/cycle}$$
$$\text{GPC@89 } ^\circ\text{C} = 0.41 \text{ \AA/cycle}$$



# LiHMDS (Li-Si-O by [LiHMDS + O<sub>3</sub>])

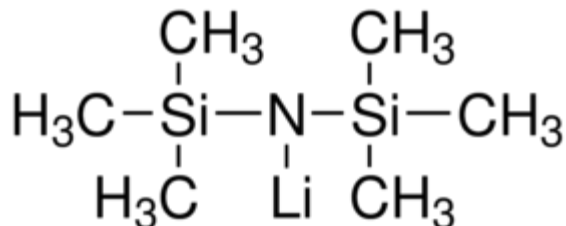
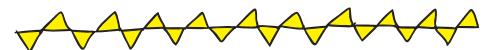


FIG. 7. (Color online) Photographs of the soda lime glass substrate after ALD lithium silicate film deposition at 300 °C.

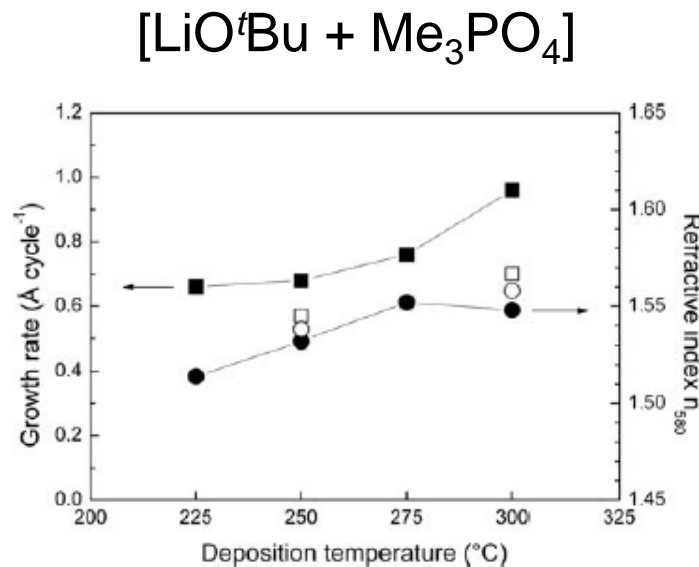
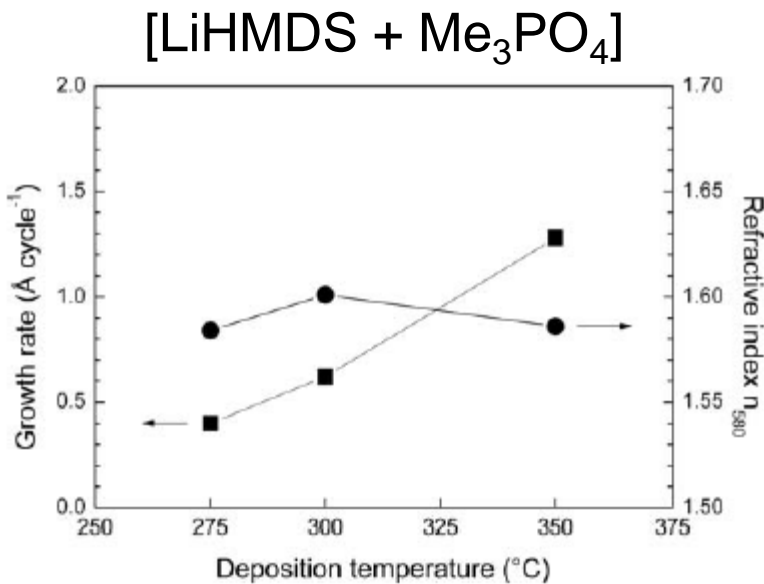
TABLE I. Elemental compositions of the lithium silicate thin films as measured with ERDA.

	Deposition temperature					
	150 °C	200 °C	250 °C	300 °C	350 °C	400 °C
Li (at. %)	31.8	29.8	32.5	30.8	30.0	37.5
Si (at. %)	11.2	13.9	16.1	17.7	18.5	15.1
O (at. %)	44.2	48.7	46.3	48.6	49.6	45.9
C (at. %)	3.94	0.96	0.65	0.32	0.14	0.15
H (at. %)	8.78	6.63	4.60	2.70	1.71	1.29
Thickness (nm)	62	62	86	120	140	172
Density (g/cm <sup>3</sup> )	2.48	2.26	2.32	2.36	2.39	2.5
Li:Si:O ratio	2.8:1:4.0	2.1:1:3.5	2.0:1:2.9	1.7:1:2.8	1.6:1:2.7	2.5:1:3.0

Li-content decreased with increasing temperature

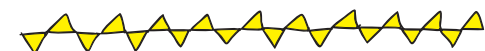


# $\text{Li}_3\text{PO}_4$



J. Hämäläinen, ... M. Leskelä, *J. Electrochem. Soc.* **159** (2012) A259.

**Figure 2.** Growth rates and refractive indexes of lithium phosphate films as a function of deposition temperature. The precursor pulses and purges were either 2 s (open symbol) or 4 s (solid) each. A total of 1000 cycles were applied for each deposition.



# LiPON

[LiO<sup>t</sup>Bu + H<sub>2</sub>O + TMP + <sup>P</sup>N<sub>2</sub>]

LiPON (250 °C), 1.05 Å/s,  
N content controlled by <sup>P</sup>N<sub>2</sub> pulse length.

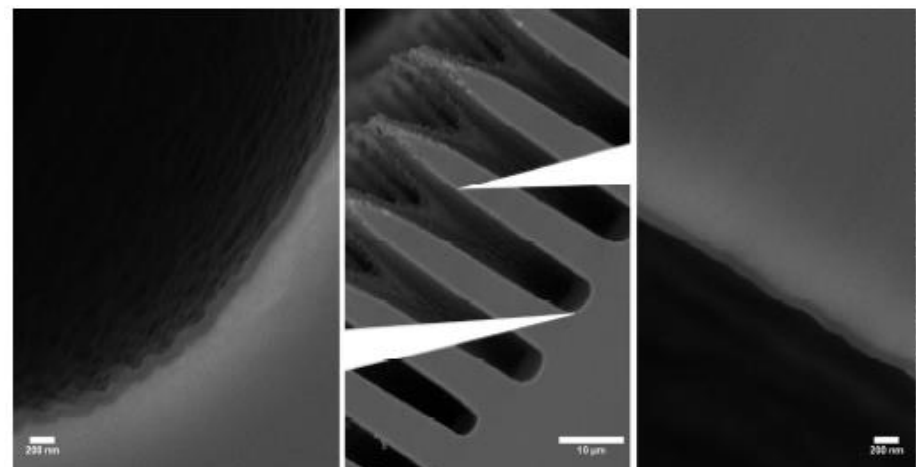
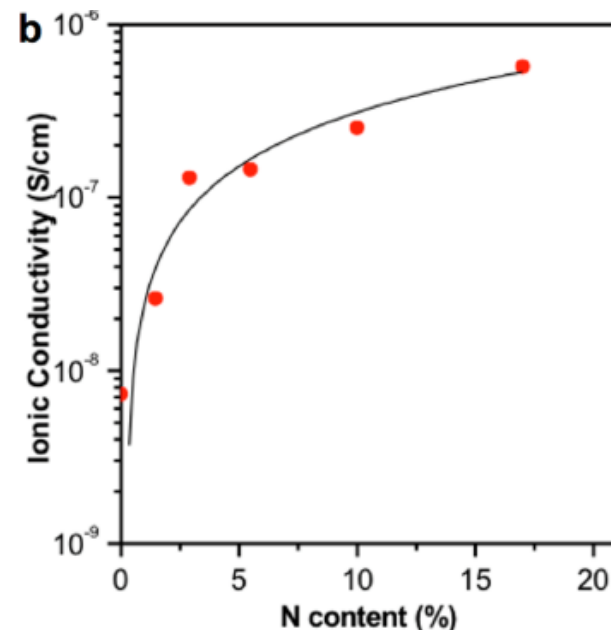
A. C. Kozen, A. J. Pearse, C.-F. Lin, M. Noked G. W. Rubloff, *Chemistry of Materials*, 2015, 27, 5324-5331.

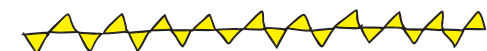
[(H<sub>2</sub>NP(O)(OC<sub>2</sub>H<sub>5</sub>)<sub>2</sub>) + LiHMDS]

LiPON (250 – 330 °C), 0.7 – 1.0 Å/s.

Ionic conductivity of  
 $6.6 \times 10^{-7}$  Scm<sup>-1</sup> @ RT.

M. Nisula, Y. Shindo, H. Koga M. Karppinen, *Chemistry of Materials*, 2015, 27, 6987-6993.





# LiAlO<sub>2</sub>

[LiO<sup>t</sup>Bu + H<sub>2</sub>O] + [TMA + H<sub>2</sub>O] @ 225 °C

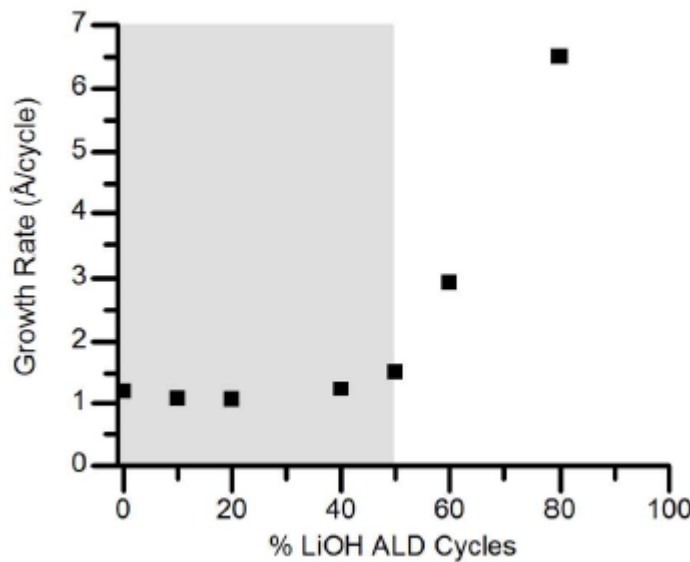


Figure 7. LiAlO<sub>x</sub> growth rate measured by ellipsometry as a function of % LiOH ALD cycles. Gray shaded area designates the region of stable growth with constant, linear growth as a function of ALD cycles.

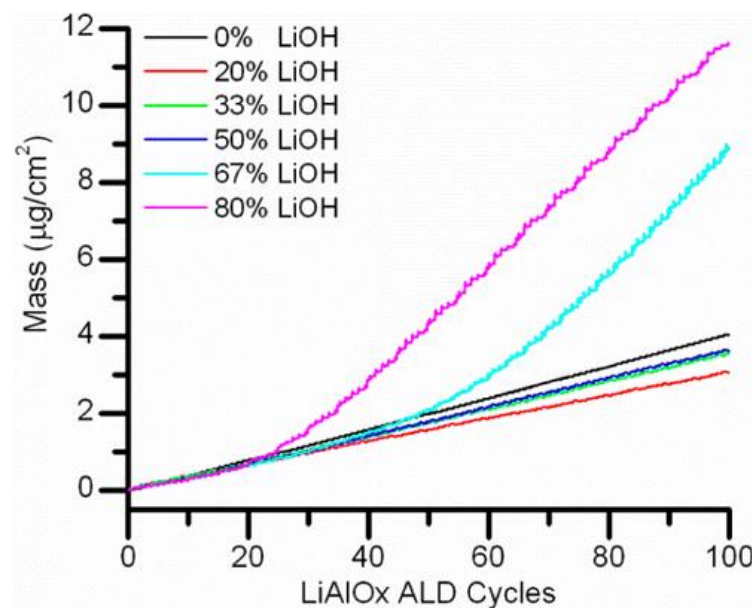
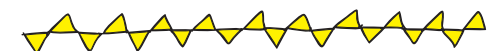


Figure 4. QCM mass gain profiles acquired over 100 cycles of LiAlO<sub>x</sub> ALD using 0%, 20%, 33%, 50%, 67%, and 80% LiOH cycles.



# LiAlO<sub>2</sub>

[LiO<sup>t</sup>Bu + H<sub>2</sub>O] + [TMA + H<sub>2</sub>O] @ 225 °C

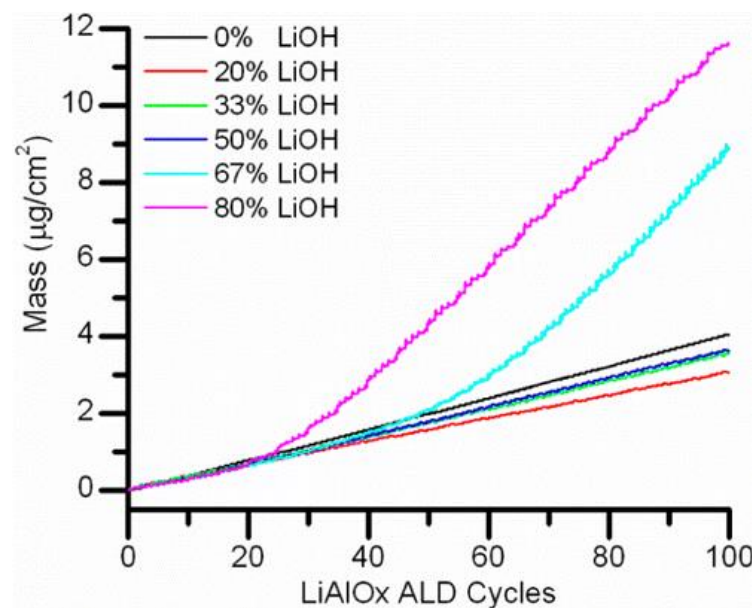
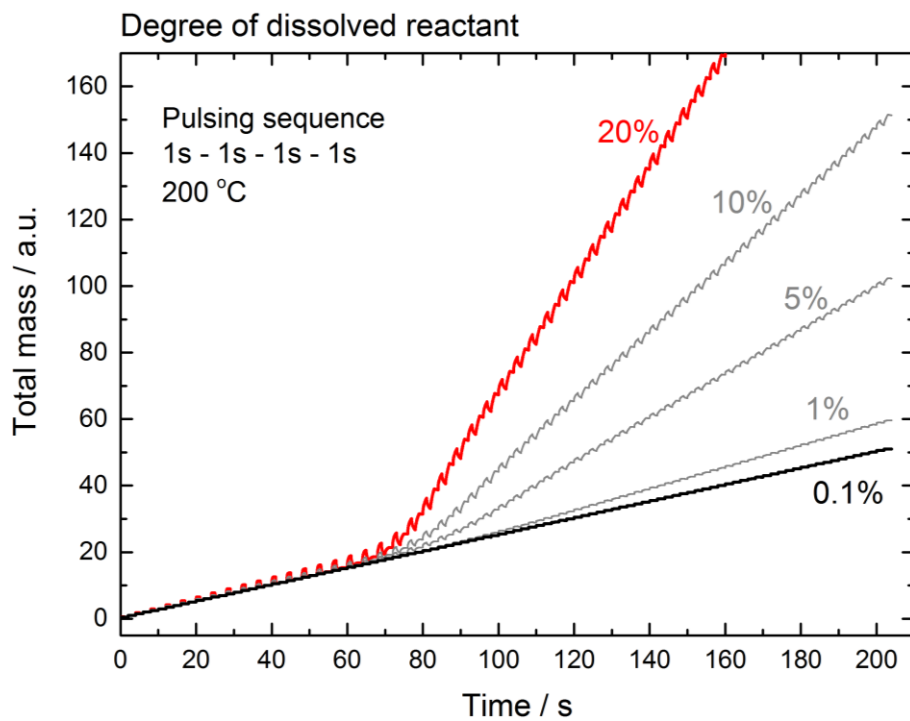
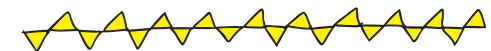


Figure 4. QCM mass gain profiles acquired over 100 cycles of LiAlOx ALD using 0%, 20%, 33%, 50%, 67%, and 80% LiOH cycles.



# LiAlO<sub>2</sub>

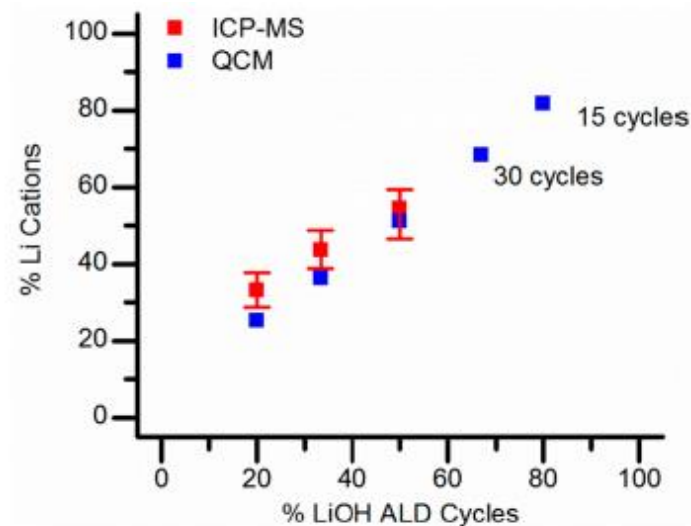
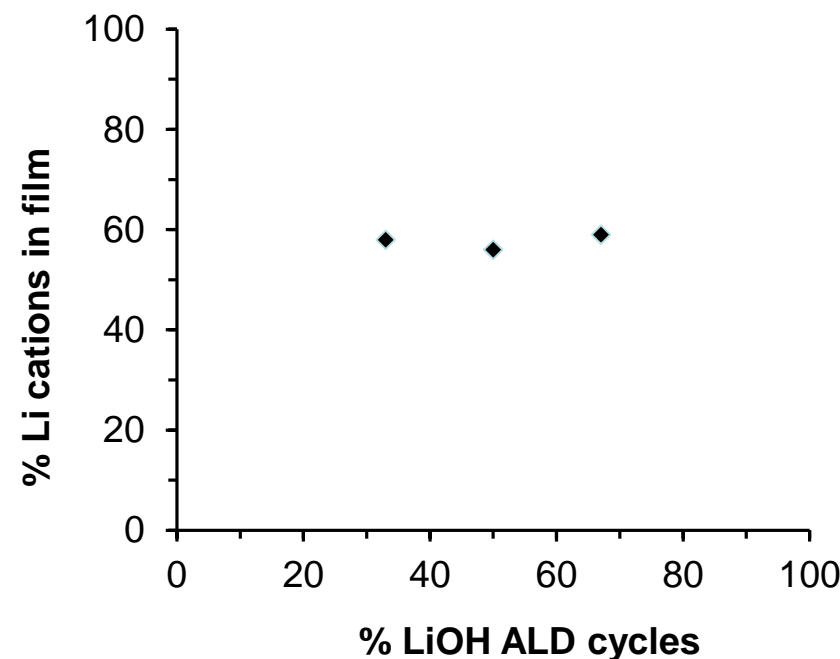
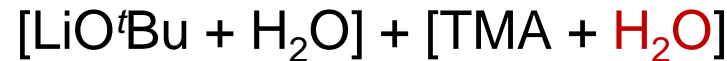
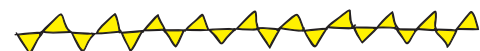


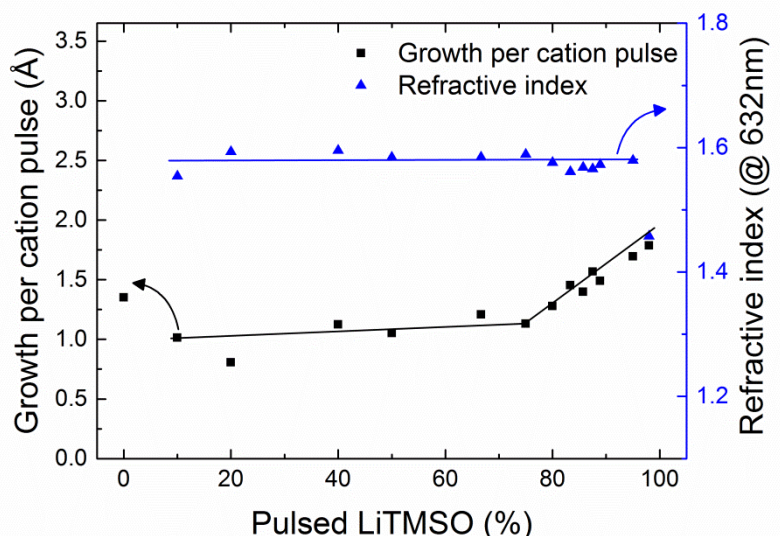
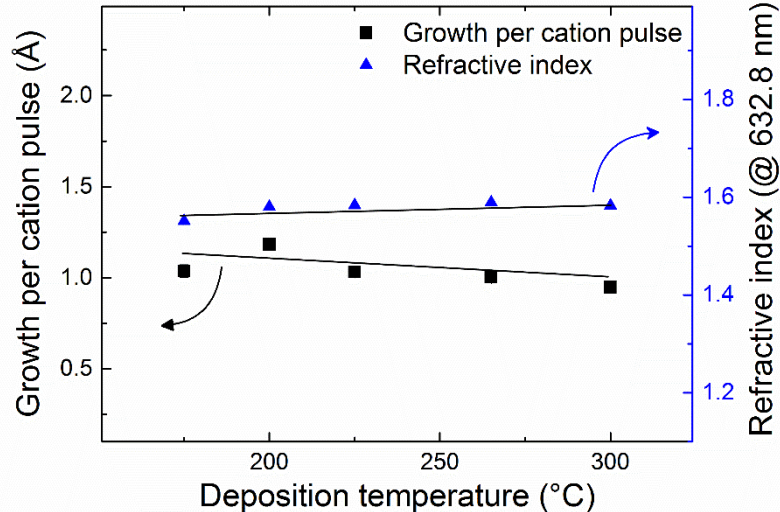
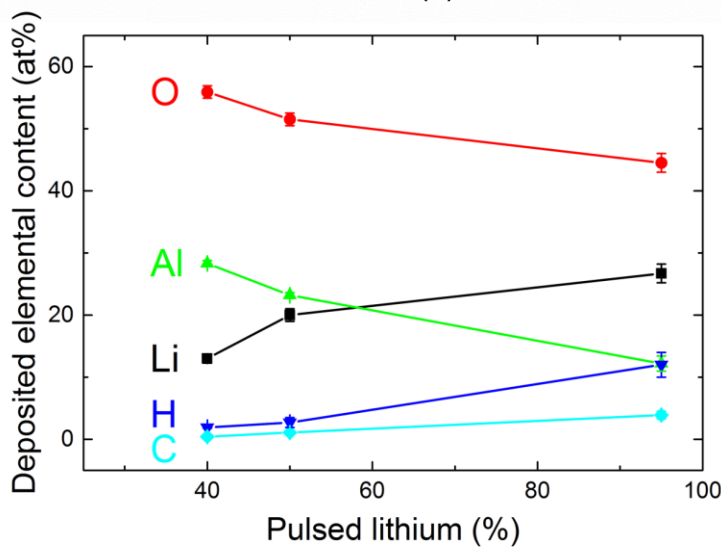
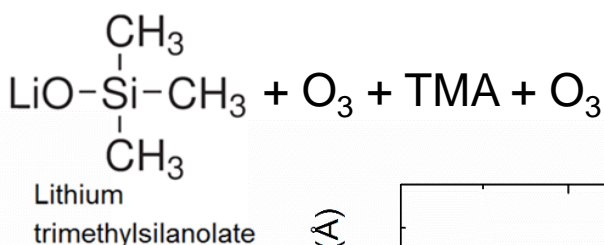
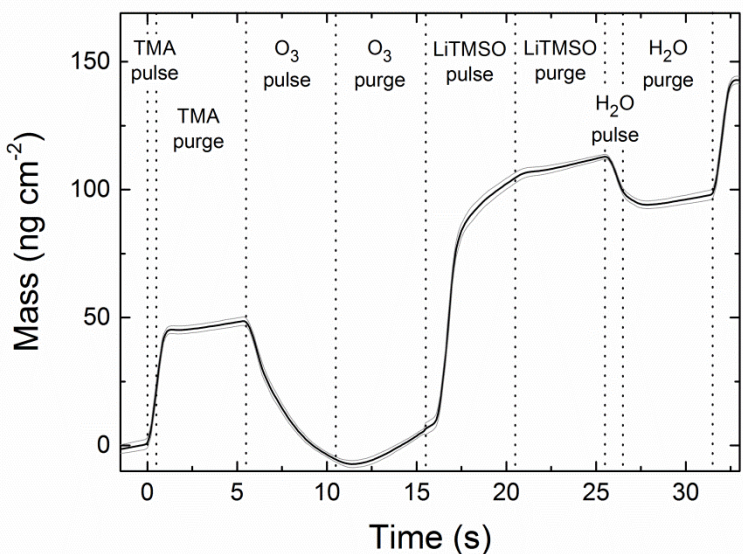
Figure 8. Li cation percentage in LiAlO<sub>x</sub> films measured by ICP-MS and QCM as a function of % LiOH ALD cycles.

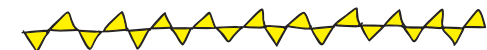
V. Mikkulainen, ... H. Fjellvåg, *J. Vac. Sci. Technol. A* **33** (2015) 01A101

D.J. Comstock, and J. W. Elam, *J. Phys. Chem. C* **117** (2013) 1677.

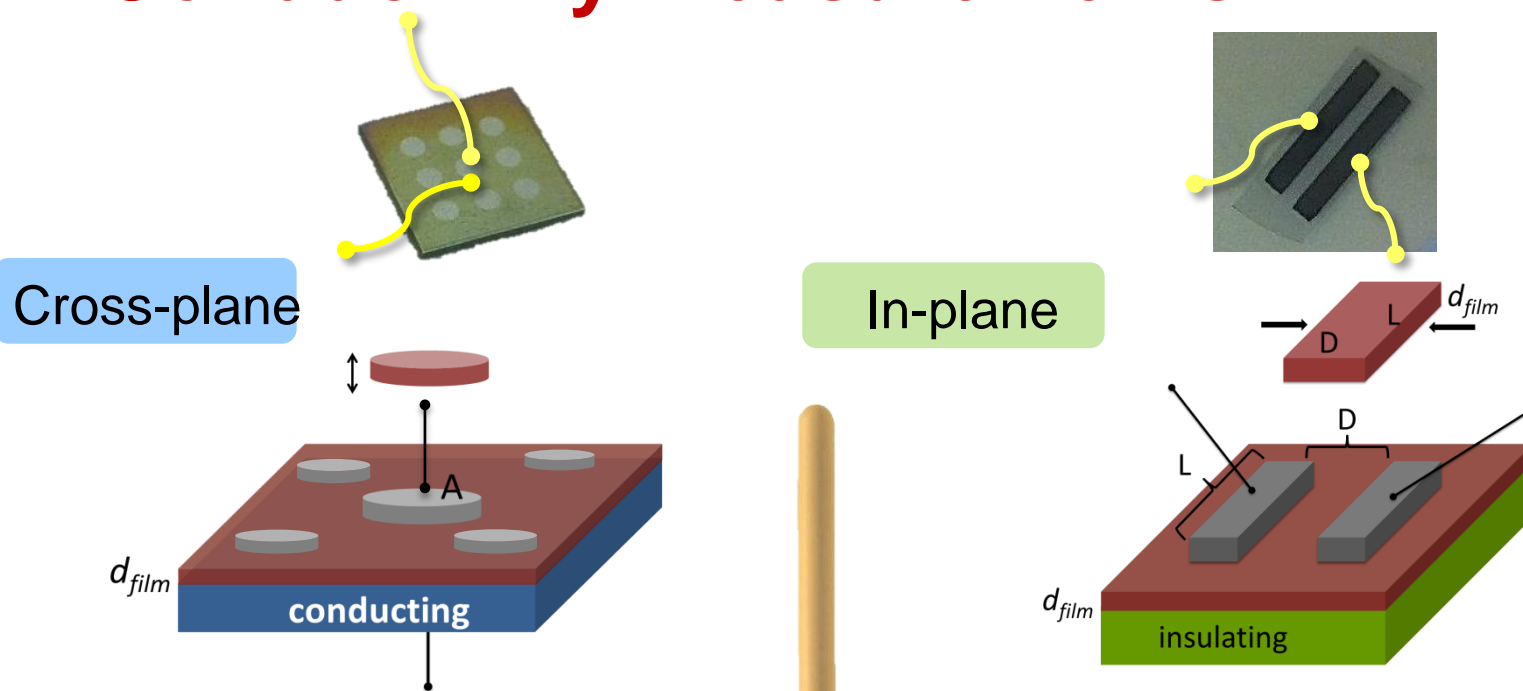


# $\text{LiAlO}_2$





# Conductivity measurements



$$\sigma_{cross} = \frac{L}{R \times A} = \frac{d_{film}}{R \times A_{electrode}}$$

- More practical interests
- Challenges: short-circuiting
- Difficult to carry out

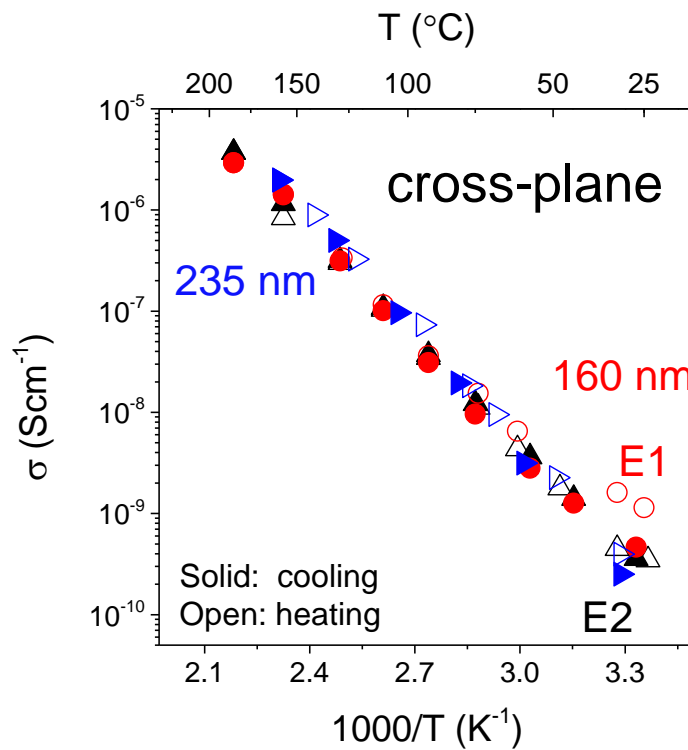
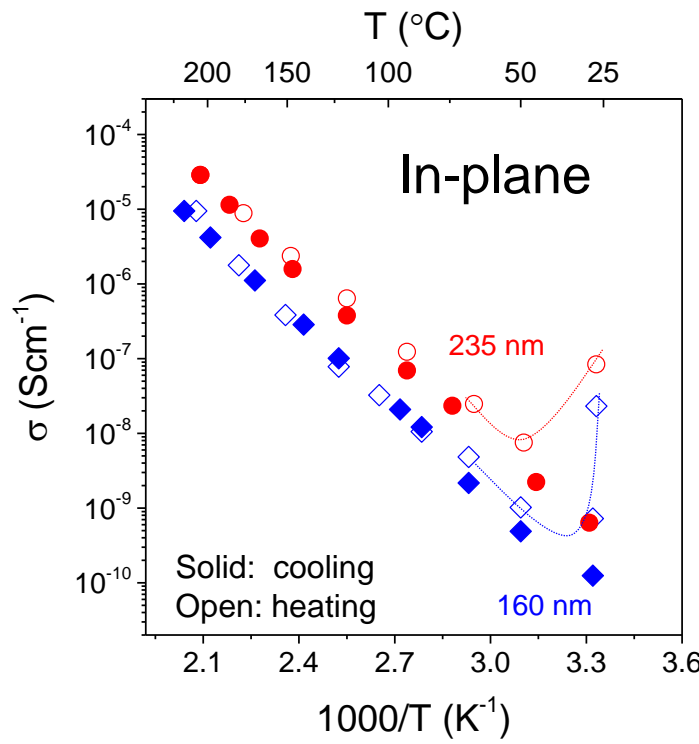


$$\sigma_{in} = \frac{L}{R \times A} = \frac{D_{electrode}}{R \times (d_{film} \times L)}$$

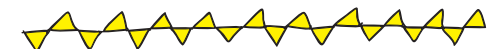
- Circumvent the short-circuitings
- Significant resistance
- More sensitive to parasitics



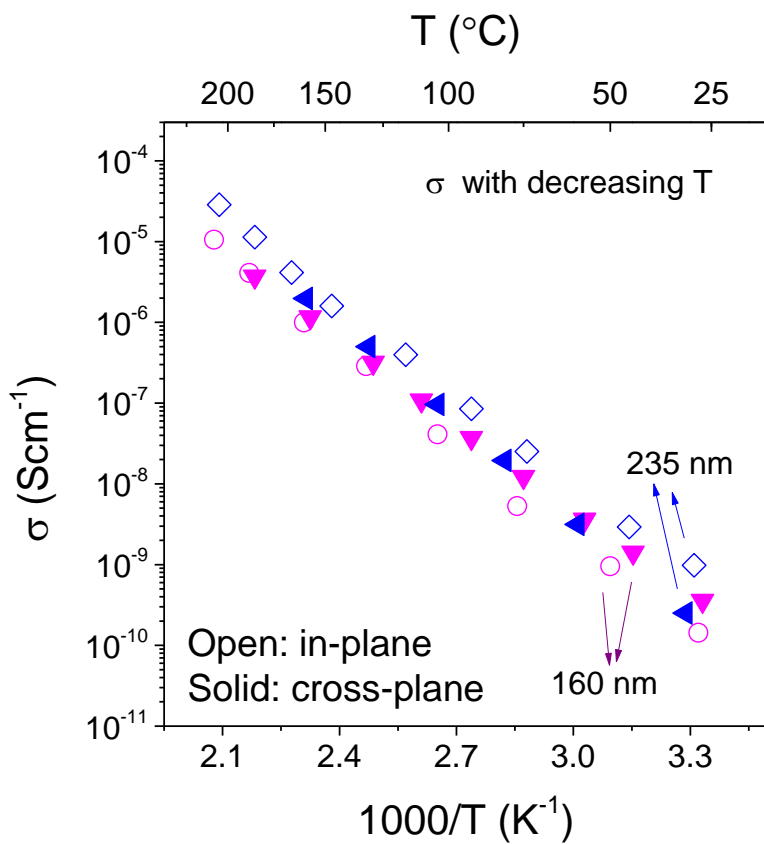
# Conductivity of LiAlO<sub>2</sub> films



- Thermally activated ionic characteristics → Arrhenius relation:  $\sigma = \frac{\sigma_0}{T} \exp\left(-\frac{E_a}{kT}\right)$
- Larger thickness-dependence for in-plane method: *surface, interface*
- $\sigma$  @ room temperature:  $10^{-10} \sim 10^{-9}$  Scm<sup>-1</sup>



# Conductivity of LiAlO<sub>2</sub> films



Materials	$\sigma_{\text{RT}}$ ( $\text{S cm}^{-1}$ )	$E_a$ (eV)	Ref.
Single-crystalline $\gamma$ -LiAlO <sub>2</sub>	$\sim 1 \times 10^{-17} *$	1.14(1)	1
Polycrystalline $\gamma$ -LiAlO <sub>2</sub>	$2 \times 10^{-14} *$	0.81 (extrinsic) 1.3 (intrinsic)	2
ALD LiAlO <sub>2</sub> film on quartz substrate	$5.6 \times 10^{-8} *$	0.56	3
Quenched glass $0.6\text{Li}_2\text{O}-0.4\text{Al}_2\text{O}_3$ $0.7\text{Li}_2\text{O}-0.3\text{Al}_2\text{O}_3$	$3 \times 10^{-11} *$ $5 \times 10^{-8} *$	0.88 0.57	4
ALD LiAlO <sub>2</sub> films, sapphire and Ti substrates	$1 \sim 5 \times 10^{-10}$	0.7~0.8	This work

- Room temperature conductivity was rarely reported
- Disordered amorphous/glassy  $\text{Li}_x\text{AlO}_y \rightarrow$  higher conductivity
- Improved conductivity can be expected with increasing Li content

# Conclusion

Cathode:

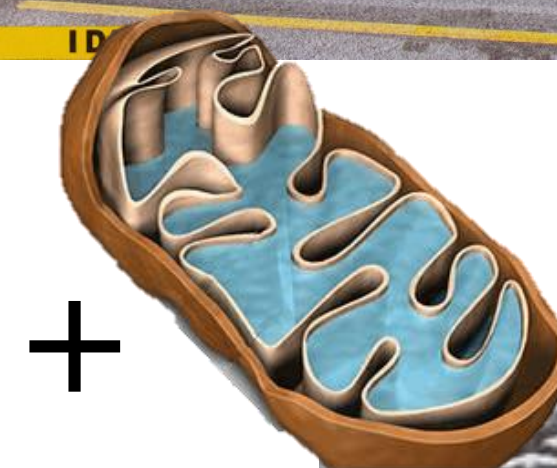
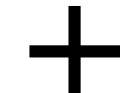
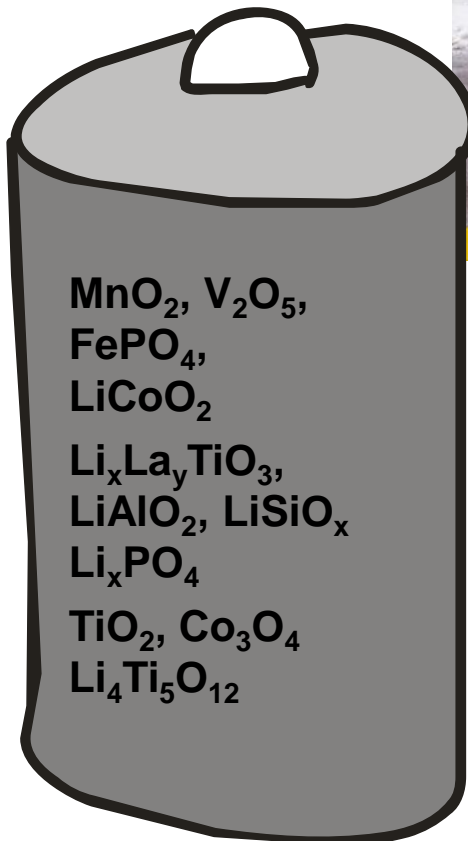
$\text{MnO}_2$ ,  $\text{V}_2\text{O}_5$ ,  
 $\text{FePO}_4$ ,  
 $\text{LiCoO}_2$

Electrolyte:

$\text{Li}_x\text{La}_y\text{TiO}_3$ ,  
 $\text{LiAlO}_2$ ,  $\text{LiSiO}_x$   
 $\text{Li}_x\text{PO}_4$

Anode:

$\text{TiO}_2$ ,  $\text{Co}_3\text{O}_4$   
 $\text{Li}_4\text{Ti}_5\text{O}_{12}$



# Acknowledgements



Helmer Fjellvåg

Mari Alnes

Matti Putkonen

Titta Aaltonen

Ville Miikkulainen

Knut B Gandrud

Erik Østreng

Anders Pettersen

Amund Ruud

Øystein S. Fjellvåg

Kenichiro Mizohata

Annina Moser

Yang Hu

Martin Sunding

Anna Magraso

Alexander Azarov

Timo Sajavaara

Leila Costelle